AD-A077 022 AIR FORCE GEOPHYSICS LAB HANSCOM AFB MA F/G 8/12
CLIMATIC CHAMBER TESTS OF A SURFACE ICE ACCRETION MEASUREMENT S--ETC(U
MAR 79 P TATTELMAN
UNCLASSIFIED AFGL-TR-79-0079 NL

1 OF 1
AD
AD A077022

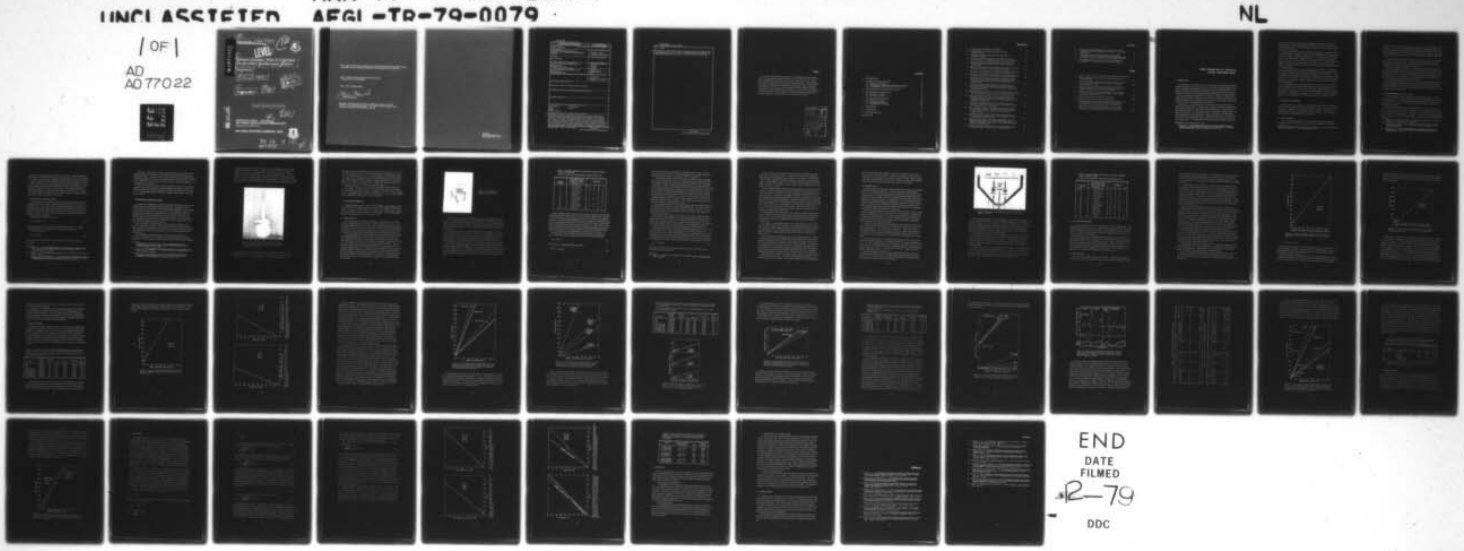

END
DATE FILMED
12-79
DDC

AFGL-TR-79-0079, AFGL-AFSG-
AIR FORCE SURVEYS IN GEOPHYSICS, NO. 406

LEVEL II

# Climatic Chamber Tests of a Surface Ice Accretion Measurement System

PAUL TATTELMAN

Final rept.



26 March 1979

50





099

16

METEOROLOGY DIVISION PROJECT 6670
AIR FORCE GEOPHYSICS LABORATORY
HANSCOM AFB, MASSACHUSETTS 01731

AIR FORCE SYSTEMS COMMAND, USAF

This report has been reviewed by the ESD Information Office (OI) and is releasable to the National Technical Information Service (NTIS).

This technical report has been reviewed and is approved for publication.

FOR THE COMMANDER

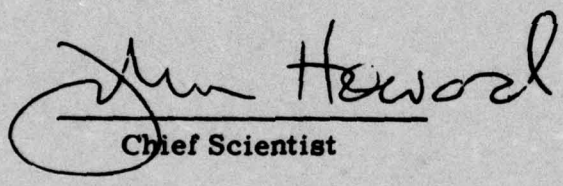

Chief Scientist

Qualified requestors may obtain additional copies from the Defense Documentation Center. All others should apply to the National Technical Information Service.

Printed by
United States Air Force
Hanscom AFB, Mass. 01731

Unclassified

SECURITY CLASSIFICATION OF THIS PAGE (When Data Entered)

| REPORT DOCUMENTATION PAGE | | READ INSTRUCTIONS BEFORE COMPLETING FORM |
|---|---|---|
| 1. REPORT NUMBER<br>AFGL-TR-79-0079 | 2. GOVT ACCESSION NO. | 3. RECIPIENT'S CATALOG NUMBER |
| 4. TITLE (and Subtitle)<br>CLIMATIC CHAMBER TESTS OF A SURFACE ICE ACCRETION MEASUREMENT SYSTEM | | 5. TYPE OF REPORT & PERIOD COVERED<br>Scientific. Final.<br>6. PERFORMING ORG. REPORT NUMBER |
| 7. AUTHOR(s)<br>Paul Tattelman | | 8. CONTRACT OR GRANT NUMBER(s) |
| 9. PERFORMING ORGANIZATION NAME AND ADDRESS<br>Air Force Geophysics Laboratory (LYD)<br>Hanscom AFB<br>Massachusetts 01731 | | 10. PROGRAM ELEMENT, PROJECT, TASK AREA & WORK UNIT NUMBERS<br>62101F<br>66700903 |
| 11. CONTROLLING OFFICE NAME AND ADDRESS<br>Air Force Geophysics Laboratory (LYD)<br>Hanscom AFB<br>Massachusetts 01731 | | 12. REPORT DATE<br>26 March 1979<br>13. NUMBER OF PAGES<br>50 |
| 14. MONITORING AGENCY NAME & ADDRESS(if different from Controlling Office) | | 15. SECURITY CLASS. (of this report)<br>Unclassified<br>15a. DECLASSIFICATION/DOWNGRADING SCHEDULE |

16. DISTRIBUTION STATEMENT (of this Report)

Approved for public release; distribution unlimited.

17. DISTRIBUTION STATEMENT (of the abstract entered in Block 20, if different from Report)

18. SUPPLEMENTARY NOTES

19. KEY WORDS (Continue on reverse side if necessary and identify by block number)

Ice accretion
Glaze
Rime
Design criteria
Ice detection
Icing

20. ABSTRACT (Continue on reverse side if necessary and identify by block number)

Climatic chamber tests of an off-the-shelf ice detection system manufactured by Rosemount Engineering Company were conducted to evaluate its capability to determine ice amounts measured on cylinders. One-hour tests were run for a variety of windspeeds, temperatures, and icing conditions. Some longer duration tests, up to 17 hours, were also performed. Analysis of the data indicates that the Rosemount system is highly correlated with the mass of ice measured on the cylinders when the data are divided into freezing rain and rime icing events. The Rosemount system is also highly correlated with

DD FORM 1 JAN 73 1473 EDITION OF 1 NOV 65 IS OBSOLETE

Unclassified

SECURITY CLASSIFICATION OF THIS PAGE (When Data Entered)

20. (Cont)

ice thickness, but without the pronounced dependence upon the type of icing. In the light of positive test results, a method is proposed for utilizing the Rosemount system for observing ice accretion at the earth's surface.

## Preface

The author is grateful to Richard Toliver, Wayne Drake, and their support group at the Armament Development and Test Center, Eglin AFB, Florida, for close cooperation in the conduct of the climatic chamber tests. Their contributions immeasurably enhanced the scope and validity of the tests. His appreciation is extended to colleagues in the Climatology and Dynamics Branch, especially Arthur Kantor, Iver Lund, and Donald Grantham, for their support and helpful suggestions. Thanks are due also to René Cormier, AFGL, for his encouragement in the initiation of this study, to William Lamkin for his support as electronics technician, and to Mrs. Helen Connell, for the typing of this report.

## Contents

## Illustrations

## Tables

# Climatic Chamber Tests of a Surface Ice Accretion Measurement System

## 1. INTRODUCTION

In this report, ice accretion, or icing, refers to ice accumulating on stationary objects located near the earth's surface. It is one of the few meteorological conditions not quantitatively observed on a routine basis by any national weather service Because icing can totally disrupt transportation, cause power and communication outages, and result in severe damage to structures bearing the burden of accumulated ice, better observation of icing events are required. A paucity of information on icing can result in high construction costs in cases of overdesign, structural failure when icing design loads are inadequate, and poor planning in locating structures that could be placed in less susceptible nearby locations.

Most of the current information on ice storms was recorded only because of extensive human distress, or a large amount of damage. Even then, measurements have usually been made on tree branches, transmission lines, or just about any other convenient surface. These observations are subjective, nonstandardized, and difficult to interpret. The most objective measurements have been made using a cable suspended between two poles with a weight-measuring device, or tensionometer, between one of the poles and the cable. This method has been used to collect data in the Soviet Union.[1] The Bonneville Power Administration, Portland, Oregon has

(Received for publication 23 March 1979)

1. Rudneva, A. V. (1961) Glazed Frost and Ice Formation on Cables Within the Territory of the USSR, Special Translation, No. ATD U-64-47, Aerospace Technology Division, Library of Congress, 28 July 1964.

many years of this type of data taken in mountain locations in the northwestern United States. Two shortcomings of this instrumentation that preclude its use at most observing sites are size and orientation, which result in ice amounts being a function of wind direction.

Ice accretion studies have been conducted by independent organizations such as power and telephone companies. However, these investigations have been limited in scope, as well as in geographic applicability. Many researchers,[2,3,4] to cite a few, have assimilated the available material on ice accretion and attempted to delineate the ice accretion hazard. Other researchers,[5,6,7,8] have attempted to relate ice accretion to readily available climatological data. However, these studies are not only limited, but they fall short of providing meaningful information for design criteria.

The bulk of the work on ice accretion explores the theoretical relationships between ice formation and the parameters affecting its rate of accumulation, density, shape, and so on (for example, Chaine and Skeates,[9] and Kuroiwa[10]). These relationships are important to a complete understanding of ice accretion processes. They are, however, based on ideal steady-state atmospheric conditions and are of limited use in calculating a realistic magnitude of ice accretion in the turbulent natural environment.

The importance of ice accretion design criteria to the Air Force is evidenced by the large number of requests from project offices requiring guidance in this area. In order to provide more reliable icing design values, it will be necessary to establish a climatology of ice accretion observations at a representative number of sites where conventional observations are also available. The first step towards this goal is the development of a method for objectively measuring ice accretion.

## 2. DYNAMICS OF ICE ACCRETION

Measurements of ice amounts are extremely difficult to make, since the shape and size of the collecting surface and its orientation to the wind give rise to wide differences. Furthermore, the configuration and density of accumulated ice on a surface are dependent on a number of atmospheric variables. This section describes the basic relationships of these parameters.

### 2.1 Types of Ice Accretion

There are three basic kinds of ice formed by accretion in the atmosphere: glaze, hard rime, and soft rime. Glaze is transparent and has a density with

---

(Because of the large number of references cited above, they will not be listed here. See Reference Page 49, for References 2 through 10.)

respect to water (units for densities are g $cm^{-3}$) of 0.8 to 0.9 (the density of pure ice is 0.917). It is formed when the time required for freezing of the drops on a surface is greater than the time interval of impingement of the drops. This occurs most often during freezing rain or drizzle, but it can also result from large supercooled cloud droplets accompanied by high windspeeds and an ambient temperature near 0°C.

Hard rime is less transparent than glaze and, at times, opaque, depending on the quantity of air trapped in the ice. It is formed when the time required for freezing of the drops on a surface is approximately equal to the time interval of impingement. The density varies from about 0.6 to 0.9.

Soft rime is both white and opaque. It is formed when the time interval for freezing of the droplets on a surface is less than the time interval of impingement. Soft rime is feathery or granular in appearance, with a density less than 0.6. Rime ice, both hard and soft, is most often formed by the freezing of supercooled cloud or fog droplets. For this reason it occurs most frequently at mountainous locations, or on land areas adjacent to bodies of water.

The adhesive strength of accreted ice on a surface is greatest when the density of the ice is high; this is because more particles are in contact with the surface. The adhesive strength of both glaze and hard rime is high, but as the ice density decreases below about 0.6, its adhesive strength becomes low enough for the ice to be shaken loose by a slight shock.

### 2.2 Meteorological Parameters Affecting Ice Accretion

The most significant meteorological parameters which interact to determine the type of icing are: drop size, temperature, windspeed, and liquid water content per unit volume of air. It has been determined experimentally[11] that ice density increases with an increase in each of these as long as the ambient temperature remains below freezing.

Raindrops with diameters greater than about 0.5 mm and with a maximum of about 5 to 6 mm will almost always produce glaze. Two main reasons are: (1) The rate of transfer of latent heat from the freezing of these large drops to the air, and the accreting surface is slow; and (2) freezing rain occurs at relatively high temperatures, rarely below -5°C.[12, 13] Drizzle drops, which have diameters between about

11. Macklin, W.C. (1961) The density and structure of ice formed by accretion, Quart. J. Roy. Meteorol. Soc. 88:30-50.

12. Bryson, R.A., and Hare, F.K. (1974) Climates of North America, World Survey of Climatology, Vol. II, Elsivier Scientific Publishing Co., Amsterdam, 420 pp.

13. Bilello, M.A. (1971) Frozen Precipitation: Its Frequency and Associated Temperatures, Cold Regions Research and Engineering Laboratory, Hanover, N.H., 13 pp.

0.2 to 0.5 mm, usually produce either glaze or hard rime. Freezing drizzle has been observed at much colder temperature than freezing rain[14] so that the density of accreted ice can vary more, depending upon the air temperature and windspeed.

Cloud, or fog droplets have diameters less than 200 $\mu$ m, but drops in the 100 to 200 $\mu$ m range are rare except in clouds that are likely to precipitate. A review of cloud droplet sizes measured experimentally[15] indicates that fog and stratus clouds have droplet sizes in the 1 to 45 $\mu$ m range. Consequently, exposure to supercooled clouds or fog will usually result in light rime. However, a combination of high windspeeds, temperatures just below freezing and, a high liquid water content can result in either glaze or hard rime.

### 2.3 Aerodynamic Factors Affecting Ice Accretion

Ice accretion measurements are extremely difficult to quantify because of the significant effect of size, shape, and orientation with respect to air flow of the accreting object. This is because air is deflected around objects in its path, and this influences the trajectories of supercooled drops in the flow. Basically, two forces act on the drops: drag force and inertial force. The drag force tends to make the drops move with the air flow, whereas the inertial force tends to make the drops move in a straight line.

The magnitude of the drag force $F_D$ is

$$F_D = \frac{\pi}{2} \rho_a C_D v^2 r^2 \tag{1}$$

where $\rho_a$ is the air density; $C_D$ the drag coefficient of the drops; v the relative velocity between the air and the drops; and r the radius of the drop.

The inertial force $F_I$ is

$$F_I = K\rho_w r^3 \frac{dv}{dt} \tag{2}$$

where $\rho_w r^3$ is the mass of the drop, and dv/dt the rate of change of relative velocity.[16]

---

14. Young, W. R. (1978) Freezing Precipitation in the Southeastern United States, Master's Thesis, Texas A&M University, Report Number CI 78-24, College Station, Texas, 123 pp.

15. Mason, B. J. (1971) The Physics of Clouds, 2nd ed., Oxford University Press, London, England.

16. Chaine, P. M., and Castonguay, G. (1974) New Approach to Radial Ice-Thickness Concept Applied to Bundle-Like Conductors, Industrial Meteorology - Study IV, Atmospheric Environment Service, Toronto, Canada, 11 pp.

From Eqs. (1) and (2) it can be seen that drop size has a greater effect on the inertial force than the drag force. Consequently, large drops are deflected less than smaller drops. As the size of the accreting object is increased, the deflection of air becomes greater and occurs for a longer distance in front of the object. These factors contribute to the drag force so that less drops per unit area impinge on a large object than a smaller one.

The term "collection efficiency," used to describe the effect of drop deflection, is defined as the ratio of the mass of drops impinging on an object in unit time to the mass of drops that would have impinged in the same time if there was no deflection.[17] The collection efficiency increases as obstacle size decreases, and drop size increases.

## 3. THE ROSEMOUNT ICE DETECTION SYSTEM

The Rosemount Engineering Company, Minneapolis, Minnesota, markets a line of ice detectors used primarily to detect ice formation in the intake portion of turbomachinery. These detectors are aerodynamically designed for use on aircraft, but they have been used to detect icing on towers. The ice detector works by the magnetostriction principle. An oscillator forces a small closed cylinder (the sensing probe) to vibrate longitudinally, parallel to its axis. It is driven at its resonant frequency when dry, but accretion of ice will cause a shift in resonance corresponding to the increase in mass of the probe. After a small preset amount of ice has accumulated, the sensor is deiced.

Hill[18] and Chaine[19] conducted tests on earlier models of Rosemount ice detectors in the natural environment. These tests were limited in scope, but they indicated that the instruments operated satisfactorily. However, they did not determine whether they could be used to estimate accurately the mass and thickness of accumulated ice.

The advantages of using a Rosemount ice detector for observation of ice accretion are: convenient size, durability, and the operation with limited human involvement. These advantages are quite attractive when compared to other methods

17. Stallabrass, J. R., and Hearty, P. F. (1967) The Icing of Cylinders in Conditions of Simulated Freezing Sea Spray, National Research Council of Canada, Ottawa, Canada, 50 pp.

18. Hill, A. N. (1973) An Objective Observation Technique for Freezing Precipitation, Laboratory Report No. 7-73, Sterling Research and Development Center, Sterling, Virginia.

19. Chaine, P. M., and Waymann, A. R. (1974) A Preliminary Performance Assessment of Rosemount Ice Detectors, Department of Environment, Atmospheric Environment Service, Toronto, Canada, 4 pp.

and devices that have been tried. It was decided to test Rosemount detectors under controlled conditions in a climatic chamber in order to evaluate its capability to measure ice accretion. Accordingly, four model 872DC ice detectors, a newer model than the ones tested previously, were purchased from Rosemount. The main reason for the choice of this model is the long strut (Figure 1). It was also necessary to purchase a model 524H controller, kept remote from the detectors, to actuate the deicing system. A multi-channel event recorder was used to count deicing cycles.

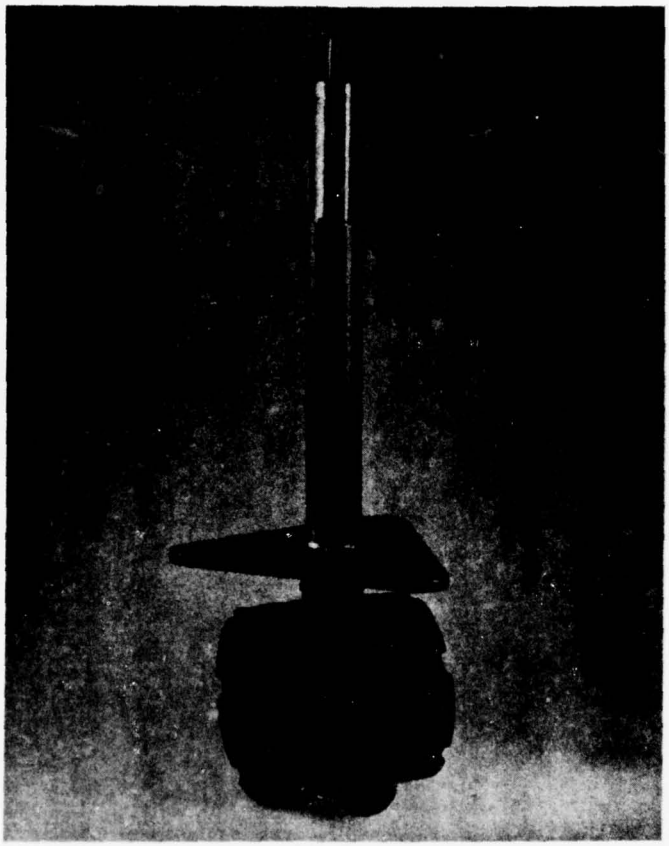

Figure 1. The Rosemount Model 872DC Ice Detector The sensing probe sits atop the 25.4 cm (10 in.) strut. During deicing, the sensor and the top 7.6 cm (3 in.) of the strut are heated

The ice detectors were calibrated at the factory to emit an icing signal when 0.5 mm (0.02 in.) of ice has accumulated on the sensing probe; however, detectors with trip points up to 5 mm are available. The sensor, cylindrical with a

hemispheric top, has a diameter of 6 mm (0.25 in.) and a length of 2.7 cm (1.1 in.). Because of its geometry, it is a very efficient collector. Although the detectors were calibrated to deice at 0.5 mm, the actual amount of ice required to trip the deice signal varies, depending on the density and distribution of ice on the sensor. After the trip point has been reached, the sensing probe and top 7.6 cm (3 in.) of the strut are deiced by an internal heater. Seven seconds after the start of the deicing cycle, the unit is ready to sense subsequent icing.

Although we obtained an event recorder to use the discrete output (that is, count the number of deicing cycles), a dc voltage recorder can be used to obtain an analog voltage output that will show the change in current as ice builds up on the sensor. It should be noted that light coatings of oil, dust, water, or other materials do not significantly affect operation of the ice detector.

## 4. THE CLIMATIC CHAMBER TESTS

Testing of the Rosemount ice detectors was conducted at the McKinley Climatic Laboratory of the Armament Development and Test Center (ADTC) at Eglin AFB, Florida. The goal was to evaluate how accurately ice accretion amounts on collectors of varying sizes could be estimated with this system. Tests were conducted during 3-week periods in May 1977 and January 1978.

### 4.1 The May 1977 Tests

The initial testing was conducted in the Engine and Equipment Test Facility. With floor dimensions of 9 × 40 m (30 × 130 ft) and a height of 7.6 m (25 ft), it is the second largest test chamber at ADTC. Steel cylinders with diameters of 3.2 mm (0.125 in.), 12.7 mm (0.5 in.), 25.4 mm (1 in.), and 50.8 mm (2 in.) (henceforth rounded to 3, 13, 25, and 50 mm, respectively), and a vertical flat plate 30.5-cm (12 in.) square were placed in close proximity to three Rosemount ice detectors.

Early in the testing, the Rosemount 872DC detectors ceased to function, owing to overheating during the deice cycle. These were returned for repair, and we were loaned 871FA detectors. The only difference between these models is the length and shape of the strut on which the sensor is mounted. These detectors were set to deice when 0.5 mm (0.02 in.) of ice accumulated on the sensor. Figure 2 shows the arrangement of instruments and collectors. Three cylinders 30.5 cm in length with diameters of 3, 13, and 50 mm (far left in Figure 2) were removable so that the mass of accreted ice could be determined. Room was not available to include vertically oriented cylinders, but previous icing tests[17] indicated that, in spite of small differences in the shape of the ice accretion as a result of gravity affecting the run-off on a vertical cylinder, no difference in collection efficiency was apparent.

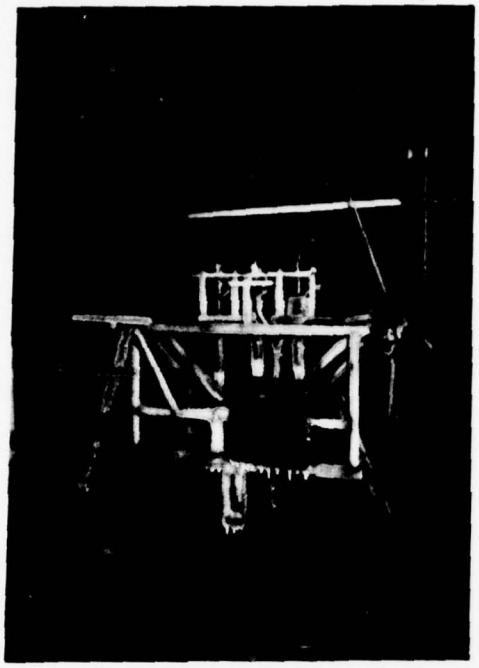

Figure 2. Arrangement of Instruments and Collectors for the May 1977 Tests

One-hour tests were run for windspeeds of 5 to 35 knots; temperatures of -1° to -7°C; freezing rainfall rates of 1.27 and 5.08 mm $hr^{-1}$ (0.05 and 0.20 in. $hr^{-1}$); and 0.2 g $m^{-3}$ water content of supercooled droplets for in-cloud icing conditions. Table 1 details the synoptic conditions. Tests were monitored from a booth on the floor of the test chamber, aside, and 3 m from the instruments and collectors on the test stand.

The wind was produced by a large electric fan with vent blades on the intake side that could be adjusted to control the windspeed. The windspeed was measured at the test stand using a hand-held 3-cup anemometer. Observation of the windspeed indicated a 6-kt fluctuation about the mean at 35 kt, which decreased to a 5-kt fluctuation about the mean at 25 kt, about 3 kt at 15 kt, and 1 to 2 kt at 5 kt.

The chamber temperature was observed using a thermocouple adjacent to the test stand with a readout in the booth, and in the control room for refrigerated air located in another part of the building. The temperature was adjusted with the wind fan on and coordinated via an audio link-up with the refrigerated-air control room. Vents for refrigerated air were located in the walls of the test chamber. Temperature fluctuations during the tests were observed to be less than 1.5°C about the mean.

Table 1. Synoptic Conditions for the One-hour Tests During the May 1977 Test Period

(Tests for which data were obtained are indicated with an X)

| Windspeed (knots) | Precipitation Rate ($mm\ hr^{-1}$) or water content for in-cloud icing ($g\ m^{-3}$) | Temperature (°C) -1 | -3 | -5 | -7 |
|---|---|---|---|---|---|
| 5 | 1.27 $mm\ hr^{-1}$ | X | X | X | X |
| 5 | 5.08 $mm\ hr^{-1}$ | X | X | X | X |
| 15 | 1.27 $mm\ hr^{-1}$ | X | X | X | X |
| 15 | 5.08 $mm\ hr^{-1}$ | X | X | X | X |
| 15 | 0.2 $g\ m^{-3}$ | | | X | X |
| 25 | 1.27 $mm\ hr^{-1}$ | X | X | X | X |
| 25 | 5.08 $mm\ hr^{-1}$ | X | X | X | X |
| 25 | 0.2 $g\ m^{-3}$ | | | X | X |
| 35 | 1.27 $mm\ hr^{-1}$ | X | X | X | X |
| 35 | 5.08 $mm\ hr^{-1}$ | X | X | X | X |
| 35 | 0.2 $g\ m^{-3}$ | | | X | X |

Rain was produced using a spray frame with nozzles chosen to yield drop sizes comparable to those of natural rain. The frame had to be situated in the chamber so that a uniform spray would be produced over the test area for each windspeed increment. This necessitated locating the spray frame upwind from the test stand. Once the spray frame was in place, it was necessary to determine the flow rate of water that would produce the desired vertical rainfall rate. Since vertical rainfall rates could not be measured due to the effect of the wind sweeping the drops horizontally across the test area, it was necessary to derive the horizontal rainfall rate across the test area corresponding to the desired vertical rain rate.

The horizontal rainfall rate ($R_H$) can be determined from the liquid water content (LWC) per unit volume and the wind velocity (V) using the expression

$$R_H = LWC \times V . \tag{3}$$

The LWC may be estimated using the expression

$$LWC = R_v \rho_w / V_T \tag{4}$$

where $R_v$ is the vertical rainfall rate, $\rho_w$ the density of water, and $V_T$ the terminal velocity of the drops. For drops of different sizes $V_T$ can be readily obtained from several sources (for example, Mason,[15] and Best[20]).

The horizontal rainfall rate was measured in the chamber with a rain gauge and a 15-cm diam pipe with a 90° bend. One open end faced horizontally into the precipitation and wind; the other was attached to the opening into the rain gauge. A flow meter, located in the booth on the chamber floor, was used to adjust the rate of water in a trial-and-error fashion until the horizontal rainfall rate measured in the rain gauge agreed with the horizontal rate calculated using Eqs. (3) and (4). The flow rate was determined in this fashion for all the rain and wind conditions. The use of Eqs. (3) and (4) and the method for measuring the horizontal rainfall rate is subject to undeterminable error, but it was our intention to produce icing conditions within the range of those occurring in nature. Since the ice detector output was compared with accumulated ice on the collectors, it was not critical to these tests that the precipitation rate be exact.

For the tests simulating in-cloud icing conditions, the water content of the air was estimated with the use of a laser particle nephelometer. The flow of water to the spray frame was adjusted to produce a water content of 0.2 g $m^{-3}$. The most frequent value of the LWC in all types of stratiform clouds is in the range of between 0.05 and 0.25 g $m^{-3}$.[15]

Drop sizes for the freezing rain and the in-cloud icing conditions were determined as follows: Silicone dielectric compound G-624 (grease) was spread over the bottom of a 6-in. glass collection dish. Dow Corning 200 fluid, a clear silicone liquid, was poured over the grease. The dish was then exposed to the precipitation. The collected drops floated in the 200 fluid and were photographed, counted and sized using a microscope with a camera attachment and a background scale.

The droplet diameters for the in-cloud conditions ranged from 10 to 90 $\mu$m with a mean of about 35 $\mu$m. This compares well with cloud and fog droplet sizes measured under natural conditions (References 15, 20). (See Section 2.2.) For the freezing rain, the mean volume drop diameter (diameter of the mean volume drop) was approximately 0.8 mm with a range of about 0.1 to 1.8 mm. The mean volume drop diameter ($D_v$) in natural rain can be estimated from the rainfall rate (I) using

$$D_v = 0.7(I)^{0.25} \tag{5}$$

where $D_v$ is in millimeters and I is in millimeters per hour. Equation (5) was derived from experimental data.[15]

---

20. Best, A.C. (1949) The size distribution of raindrops, Quart.J. Roy. Meteorol. Soc. 76:16-36.

From Eq. (5), the mean volume drop diameters for the rainfall rates used in these tests, 1.27 and 5.08 mm $hr^{-1}$, are 0.74 mm and 1.05 mm, respectively, which compares favorably with the test conditions. The range of drop diameters normally found at these rainfall rates is between 0.2 to 3.0 mm, so that the drop sizes in our freezing rain tests do not contain the full range of drop sizes found in nature. However, the contribution to the total water mass in natural rain of drops larger than 2 mm, is small.

Water entering the spray frames was refrigerated prior to reaching the climatic chamber so that its temperature on leaving the nozzles could be reduced as close to 0°C as possible. Unfortunately, the only temperature measurement of the water was made prior to its entry into the chamber. However, the water was cooled further upon flowing through hoses and the spray frame in the chamber. The magnitude of additional cooling was dependent on the ambient temperature in the chamber and the rate of water flow. There was little doubt that the water leaving the nozzles was very close to 0°C since icing caused some of the nozzles to restrict or stop the flow. This was the major cause of aborted tests. When this occurred, it was necessary to deice the nozzles and raise the temperature of the water prior to its flow into the chamber until icing ceased.

The spray frame used to simulate in-cloud conditions employed steam jackets around all nozzles to keep them from icing up, since the water flow was very low. In spite of this, nozzles froze during the colder tests, had to be deiced, and the temperature of the water to the chamber had to be raised until the freezing of nozzles ceased.

The amount of cooling of the drops from the nozzles until their impact on the collectors and ice detectors is not known. This actually varied, since the distance that the drops traveled changed as the distance of the spray frames from the test area was adjusted to suit the individual test requirements. It would be safe to assume, however, that the temperature of the drops at the test stand was very close to 0°C.

At the conclusion of each one-hour test, for the conditions outlined in Table 1, the mass of ice on the three removable cylinders was determined. The maximum radial ice thickness, from the surface of the cylinder to the edge of the accreted ice, was measured for the removable cylinders and the flat plate. The shape and color of the ice was also recorded. In order to ascertain if icing was uniform on all components, ice thickness was measured at eight points on a 25-mm diam pipe 20 cm above and 38 cm behind the detectors (see Figure 2) and on a rectangular arrangement of 25-mm diam pipe shown just below and in front of the detectors.

Measurements of ice density were made using a 3-mm diam cylinder connected to the axis of an electric motor. The slowly rotating cylinder collected ice at a fairly even rate so that the volume of ice could be estimated from simple geometry.

The ice coated cylinder was weighed in order to determine the mass of the ice. This method was used by Macklin[11] to determine ice densities. Since the motor frequently froze, and in some of the tests the deposit was lumpy, density measurements were not obtained for most of the tests. However, enough density measurements were made to indicate the range of ice-densities for our tests.

### 4.2 The January 1978 Tests

The first round of testing involved several problems that limited our capability to evaluate the Rosemount detectors. The most important of these problems follows: (1) The strut on which the sensor is located was not long enough to keep accumulated ice on the mounting plate from interfering with the flow passing the sensor; (2) the area of uniform icing in many of the tests was smaller than the area covered by the collectors and the instrumentation; (3) the vertical flat plate (see Figure 2) caused enough turbulence at windspeeds in excess of 15 knots to interfere with ice accretion on other components where ice amounts were measured; and (4) frictional heating of the air drawn through the wind machine at low windspeeds caused erratic temperature fluctuations of up to 2°C.

The second round of tests were conducted in the main chamber at ADTC, which has floor dimensions of 61 × 77 m (201 × 252 ft). This enabled us to eliminate the problem of frictional heating of air through the wind machine at low speeds, since it could be moved further from the test stand; this was preferable to closing the intake vent for the production of low speeds. Also, the windspeed could be kept more constant than in the smaller chamber.

In order to make certain that all components on the test stand were within the area of uniform icing, measurements of ice thickness and mass were made on four horizontal cylinders, 3, 13, 25, and 50 mm in diameter. These were located approximately 30.5 cm (12 in.) behind and 15.2 cm (6 in.) above the sensors on the ice detectors. This arrangement eliminated turbulence caused by the clutter of collectors in the first round of testing. Figure 3 shows the arrangement on the test stand.

For the second test period, two 872DC detectors and one 871FA detector were used. One-hour tests were run for windspeeds of calm to 35 knots, temperatures of -1°C to -10°C, freezing rain rates of 1.27 and 2.54 mm (0.05 and 0.10 in.) $hr^{-1}$, and 0.1 and 0.2 g $m^{-3}$ water content for in-cloud icing conditions. Additional longer duration tests, some with varying conditions, were also run. Table 2 details the synoptic conditions for the 1-hr tests.

The ambient chamber temperature and the windspeed were determined in the same manner as the May 1977 tests. Temperature fluctuations were observed to be less than 0.5°C about the mean. Windspeed fluctuations were about 30 percent less than those noted during the earlier test period.

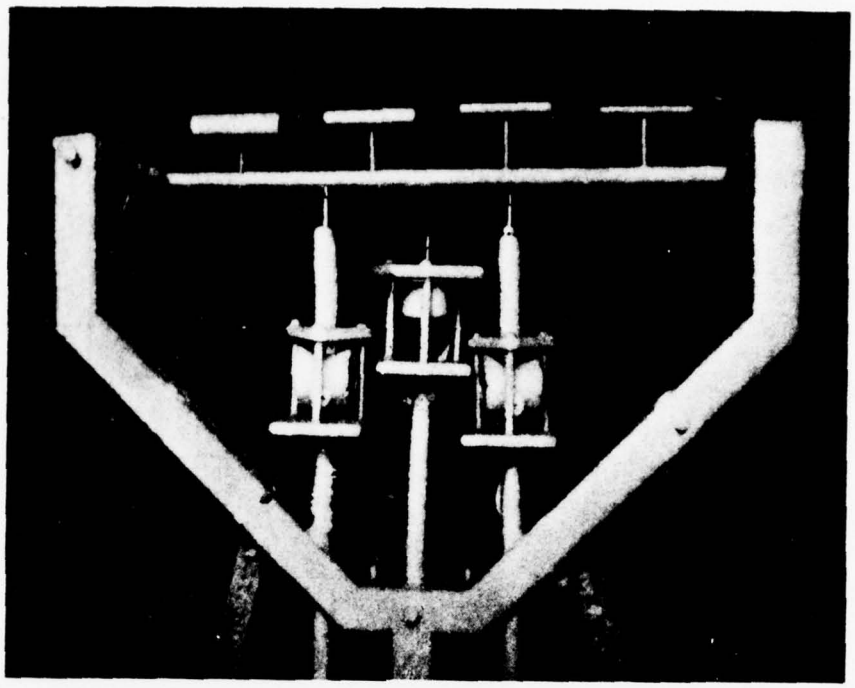

Figure 3. Arrangement of Instruments and Collectors for the January 1978 Tests

Rain and associated drop sizes were produced in the same manner as described for the original tests. Rainfall rates were calibrated using the same methods as previously, but at the lower rainfall rate, for the low windspeed tests, the rate was determined using the average of measurements from three rain gauges placed in the test area without the pipe attachment. This allowed direct measurement of rainfall rates to calibrate the flow of water for these tests. Water content during the in-cloud icing tests was determined as before.

Drop sizes were measured in the same manner as the May 1977 tests. Since the same nozzles were used in the spray frames, the size distributions for the rain and the in-cloud icing conditions were the same. The temperature of the water leaving the nozzles was reduced as close to 0°C as possible without icing of the nozzles, although this continued to be a cause of aborted tests at the lower ambient air temperatures.

At the conclusion of each test, measurements were made of the maximum radial ice thickness, the vertical dimension of the ice coated collector, and the mass of the ice for each of the four cylinders. The color and shape of the ice formation was also noted. Measurements of ice density were not made because of the high error potential as well as the problems encountered in the original tests.

Table 2. Synoptic Conditions for the One-hour Tests During the January 1978 Test Period

(Tests for which data were obtained are indicated with an X)

| Windspeed (knots) | Precipitation Rate ($mm\ hr^{-1}$) or water content for in-cloud icing ($g\ m^{-3}$) | Temperature (°C) -1 | -4 | -7 | -10 |
|---|---|---|---|---|---|
| Calm | 2.54 $mm\ hr^{-1}$ | X | X | X | |
| 5 | 1.27 $mm\ hr^{-1}$ | X | X | X | |
| 5 | 2.54 $mm\ hr^{-1}$ | X | X | X | |
| 15 | 2.54 $mm\ hr^{-1}$ | X | X | X | |
| 15 | 0.1 $g\ m^{-3}$ | X | X | X | |
| 15 | 0.2 $g\ m^{-3}$ | X | X | X | |
| 25 | 1.27 $mm\ hr^{-1}$ | X | X | X | |
| 25 | 2.54 $mm\ hr^{-1}$ | X | X | X | |
| 25 | 0.1 $g\ m^{-3}$ | X | X | X | |
| 25 | 0.2 $g\ m^{-3}$ | X | X | X | X |
| 35 | 2.54 $mm\ hr^{-1}$ | X | X | X | |
| 35 | 0.1 $g\ m^{-3}$ | X | X | X | X |
| 35 | 0.2 $g\ m^{-3}$ | X | X | X | X |

## 5. ANALYSIS OF TEST RESULTS

As pointed out in Section 4, the Model 872DC ice detectors malfunctioned at the beginning of the first test period. A Rosemount representative came to ADTC with 871FA ice detectors, the one model available on short notice for use as a replacement. The difference between the two models is in configuration only; other operating characteristics are identical.

Rosemount gave a twofold explanation for the 872DC detector failure; namely, there was no thermostat for the protection of heater coils and sensor element; and the stainless steel strut was an inadequate conductor of the heat produced. These deficiencies resulted in damage to the internal heater. However, changes have been made which incorporate a thermostat for limiting internal temperatures; and the use of nickel in place of stainless steel for the strut. In the meantime, our detectors were repaired for use during the second test period.

### 5.1 The May 1977 Tests

Our choice of the 872DC detector for evaluation as a potential instrument for measuring ice accretion was predicated on the availability of the long strut elevating

the sensor 25 cm from the mounting plate. This should keep ice accumulations on the mounting plate from influencing the flow past the sensor. On the 871A ice detector, the sensor is elevated only 5 cm above the mounting plate; as a result, ice accumulations on the mounting plate frequently interfered with the flow passing the sensor.

Measurements of ice thickness were made at eight diverse locations on the 25-mm diam pipe discussed in Section 4.1, which circumscribes the instruments and collectors. These indicate that icing rates were not uniform during many of the tests. Two factors responsible were: First, the area within which icing was uniform was not quite large enough to include all components; second, the three removable cylinders, and especially the flat plate, caused enough turbulence to influence the rate of accretion on the 25-mm pipe below the ice detectors. The net result was that this influence degraded some of the measurements on the collectors, but this was minimized by averaging some measurements, and discarding those that were obviously erroneous.

In spite of these shortcomings, the least-squares linear regression of the number of detector cycles versus the thickness of ice on the 25-mm cylinder (pipe) for thirty-eight 1-hr tests has an average correlation for the three detectors of 0.91, although the standard error of estimate (SEE) of 4.0 mm is quite large. The ice thickness for each test is the average of the four measurements judged to be the most representative. The regression line and the scatter of the points are shown in Figure 4. The linear correlations of the number of cycles of the individual detectors versus the average thickness of the same four points on the 25-mm cylinder for the thirty-eight tests are 0.90, 0.92, and 0.90, with respective SEE's of 4.4 mm, 3.8 mm, and 4.4 mm. Differences in the slopes of the regression lines are negligible. Results for the other cylinder sizes were similar.

The least-squares linear regression of the number of detector cycles versus the mass of ice measured on the 3-, 13-, and 50-mm cylinders had correlations of 0.91, 0.91, and 0.92, respectively. The respective SEE's, 138.3, 128.0, and 132.9 g reflect the large scatter of the points. This can be seen in Figure 5 which shows the points for the individual tests of the mass of ice on the 50-mm diam cylinder versus the number of instrument cycles.

These statistics indicate that ice detectors are capable of assessing ice thickness and mass for a wide range of icing rates. The large SEE's probably reflect the lack of homogeneity of icing conditions, and the interference in flow to the detectors caused by the ice buildup on their mounting plates.

A linear stepwise regression program was run to determine if the variance of the linear regression for the mass of ice could be significantly decreased by inclusion of other parameters, in addition to the number of instrument cycles. In the equation

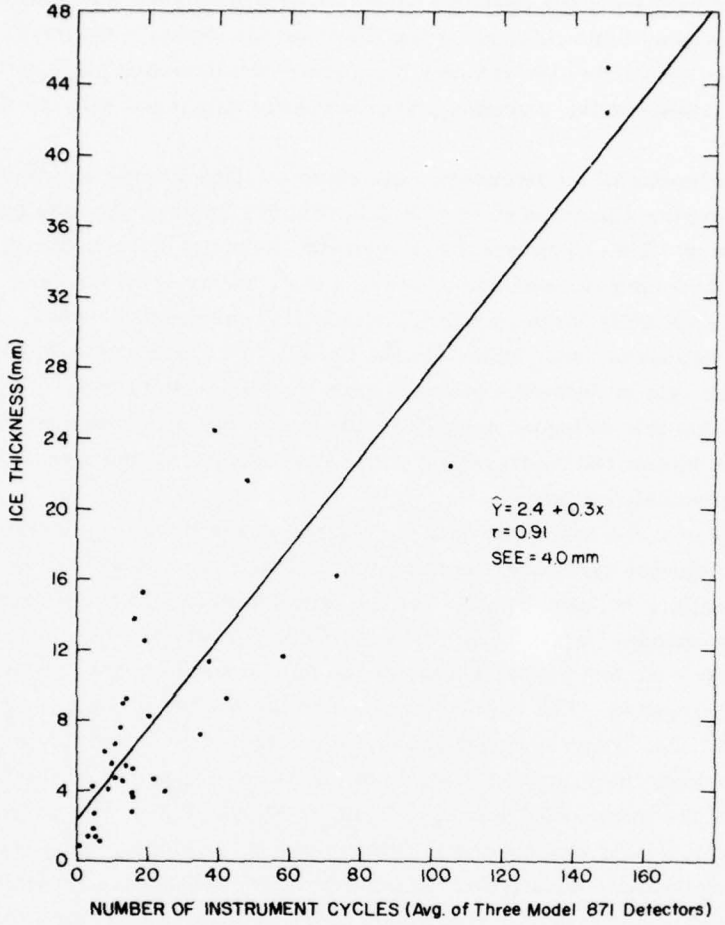


Figure 4. Linear Least-Squares Regression of the Number of Detector Deicing Cycles vs Ice Thickness on the 25-mm diam Cylinder

$$\hat{Y} = a + bx_1 + cx_2 + dx_3 + \ldots \quad (6)$$

$\hat{Y}$ represents an estimate of the mass of ice measured on one of the cylinders, $x_1$ is the parameter most highly correlated with $\hat{Y}$, $x_2$ is the parameter, among the remaining parameters, which in combination with $x_1$, contributes the most to decreasing the variance, and so forth.

Given a choice of 17 parameters, the number of instrument cycles was chosen as the one most highly correlated for all three cylinders for which measurements of ice mass were made. From among the remaining parameters, —windspeed,

temperature, liquid water content, and other formats using these three, the wind-speed was chosen as $x_2$. The reduction in variance, however, was not significant enough to warrant the use of more than one predictor, namely, instrument cycles, in Eq. (6) to obtain $\hat{Y}$.

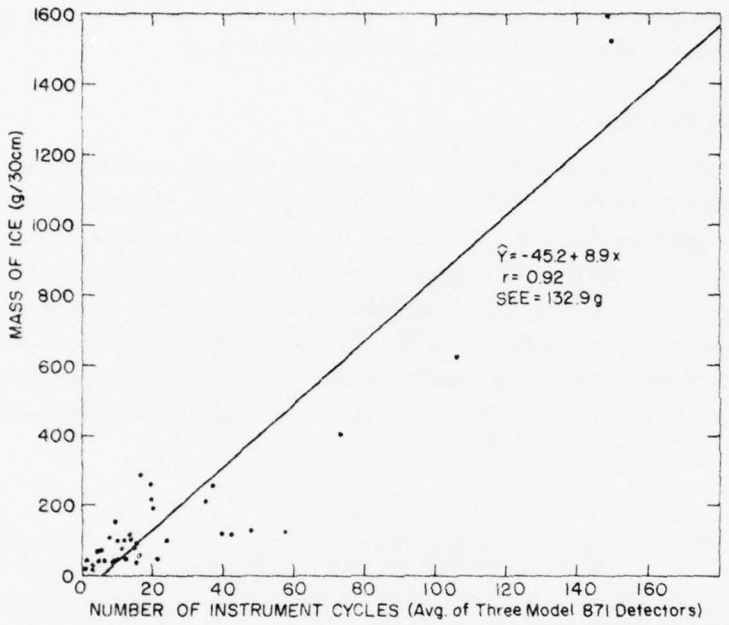


Figure 5. Linear Least-Squares Regression of the Number of Detector Deicing Cycles vs the Mass of Ice Measured on the 50-mm diam Cylinder

Measurements of ice density were made with some difficulty as noted in Section 4.1. The density, calculated for seventeen of the thirty-eight 1-hr tests, ranged from 0.63 to 0.89 g $cm^{-3}$. These measurements were not considered precise enough to be included in any of our analyses. However, the appearance of the ice, directly related to the density, was categorized as either clear, cloudy, or milky, at the conclusion of each test. Results show that clear ice formed for all tests run at a temperature of -1°C. At -3°C, the appearance of the ice was equally divided between clear and cloudy. At -5°C, cloudy ice resulted for all the freezing rain tests except one which was milky. At -7°C, milky ice resulted for all the freezing rain tests except one which was cloudy. For the in-cloud icing tests, which were run at -5° and -7°C, the appearance of the ice was milky. These results exemplify

the trend toward lower density ice at lower temperatures and smaller drop sizes used for the in-cloud icing tests.

In summary, several problems were encountered during the May 1977 tests. The most significant of these was the ice buildup on the mounting plate of the detectors which caused them to respond erratically. However, the high linear correlation between the number of instrument cycles and the mass and thickness of the ice measured on the cylinders was encouraging. Accordingly, plans were made for further testing, utilizing the 872DC detectors.

### 5.2 The January 1978 Tests

During this test period a total of forty-two 1-hr tests were run, one half with freezing rain; and the other half with in-cloud icing. The synoptic conditions for the tests are contained in Table 2. Linear least-squares regression information for the mass of ice per 30-cm length on the 25-mm diam cylinder versus the number of instrument cycles for each of the three detectors is contained in Table 3. Presented separately in the table are the regressions for the in-cloud icing and freezing rain tests. The information provided in Table 3 reveals the marked improvement in correlations and SEE's by separating the in-cloud icing and freezing rain data.

Table 3. Linear Least-Squares Regression Information for the Mass of Ice on the 25-mm diam Cylinder vs the Number of Instrument Cycles for Each Detector

(Results are given for all the test points and for the freezing rain and in-cloud icing conditions separately)

| Conditions | Detector Number Model | Number of Test Points | Slope | Y Intercept | Correlation (r) | SEE (grams) |
|---|---|---|---|---|---|---|
| All | 1/872DC | 42 | 3.44 | 10.29 | 0.80 | 29.2 |
| All | 2/871FA | 41 | 3.66 | 7.42 | 0.80 | 29.6 |
| All | 3/872DC | 42 | 4.32 | 8.94 | 0.79 | 29.8 |
| In-cloud icing | 1/872DC | 21 | 1.89 | 9.52 | 0.92 | 8.9 |
| In-cloud icing | 2/871FA | 20 | 1.94 | 8.12 | 0.93 | 8.3 |
| In-cloud icing | 3/872DC | 21 | 2.38 | 8.99 | 0.94 | 7.9 |
| Freezing rain | 1/872DC | 21 | 5.33 | 11.43 | 0.99 | 9.4 |
| Freezing rain | 2/871FA | 21 | 5.75 | 5.11 | 0.99 | 9.9 |
| Freezing rain | 3/872DC | 21 | 6.97 | 6.61 | 0.98 | 11.9 |

The regression lines and scatter of the individual test points for the mass of ice on the 25-mm diam cylinder versus the number of cycles for detector 1 (see Table 3 for detector number) are shown for all forty-two 1-hr tests (Figure 6) for the 21 freezing rain tests (Figure 7), and for the twenty-one in-cloud icing tests

(Figure 8). There is little difference in scatter diagrams for the other two detectors. The results of the linear regression analysis for the mass of ice on the 3, 13, and 50-mm diam cylinders were virtually the same and are, for this reason, not presented.

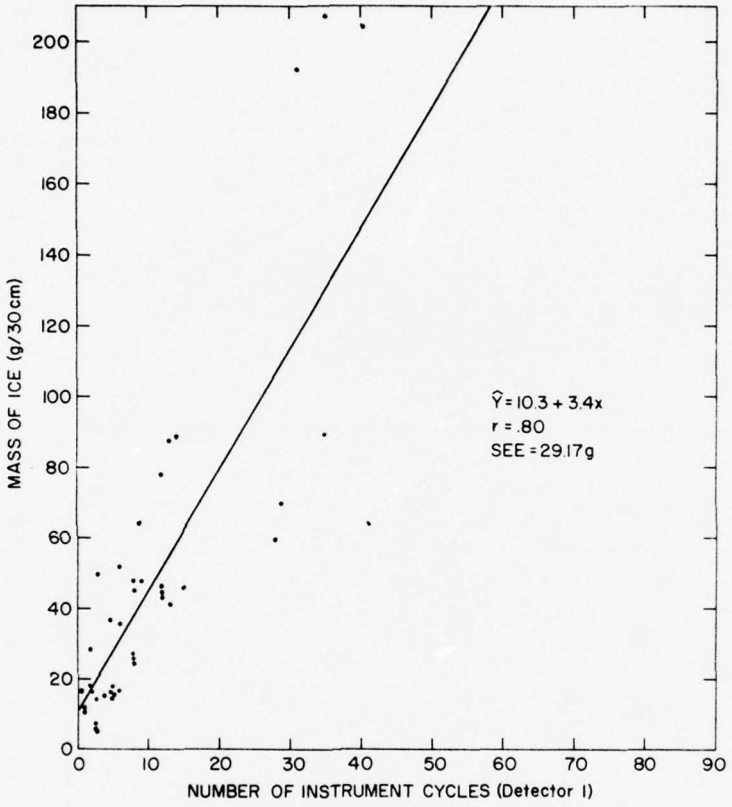


Figure 6. Mass of Ice on the 25-mm diam Cylinder vs the Number of Detector Deicing Cycles (Detector 1) for all one-hour Tests

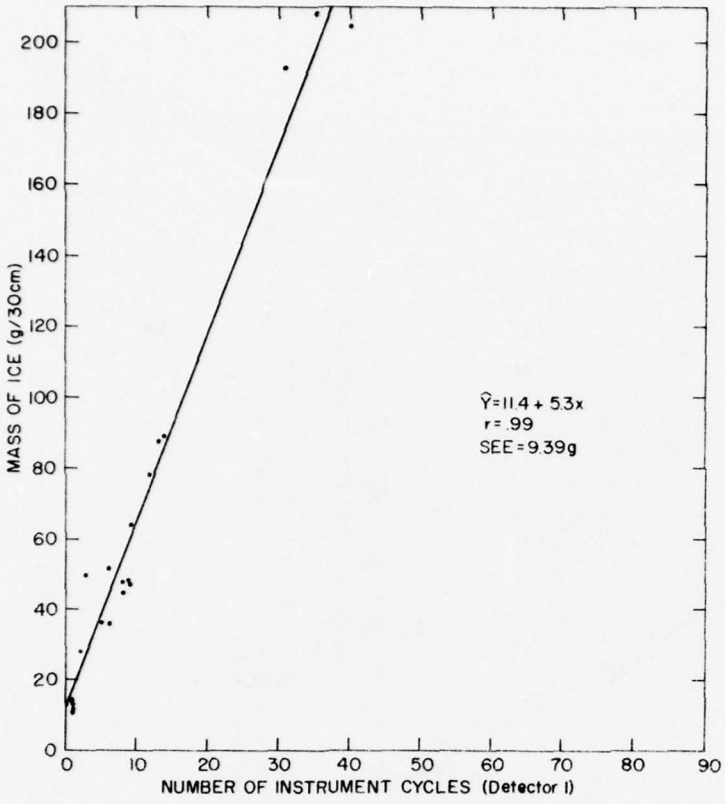


Figure 7. Mass of Ice on the 25-mm diam Cylinder vs the Number of Detector Deicing Cycles (Detector 1) for the 21 Freezing Rain Tests

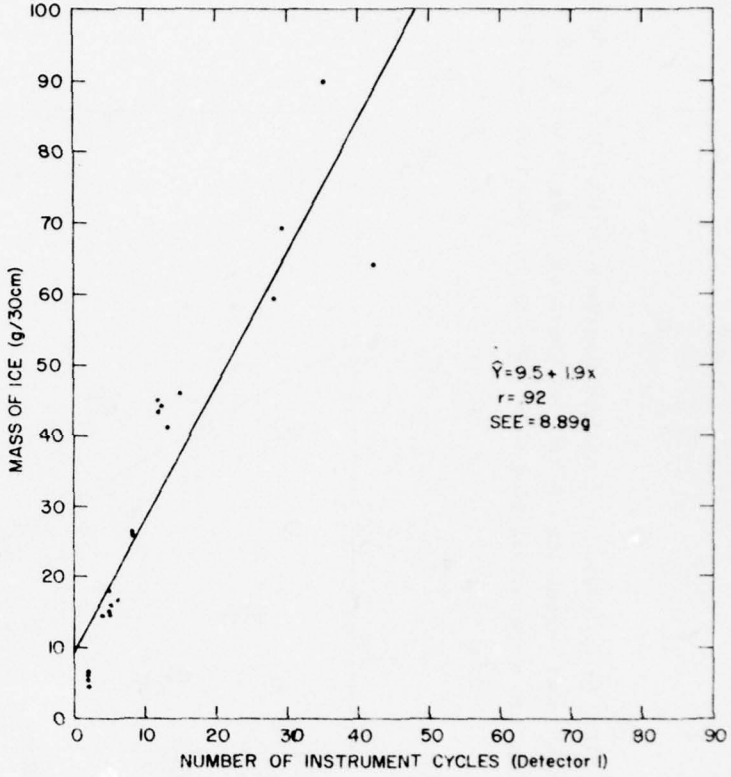


Figure 8. Mass of Ice on the 25-mm diam Cylinder vs the Number of Detector Deicing Cycles (Detector 1) for the 21 In-cloud Icing Tests

Figure 9 shows the lines for the freezing rain and in-cloud icing regression information in Table 3. It is readily apparent that, for a specific number of instrument cycles, a much greater mass of ice would accumulate on the cylinder during freezing rain than during in-cloud icing. One reason is the difference in collection efficiency for freezing rain and in-cloud icing due to difference in drop size distributions. The smaller drops associated with in-cloud icing are deflected more by the 25-mm diam cylinder than the 6-mm diam sensor on the detector. During freezing rain, the drop diameters are about 20 times greater than during in-cloud icing. These larger drops are not easily deflected due to their much greater mass. The net result would be a larger proportion of drops striking the cylinder during freezing rain then during in-cloud icing. If this were the only reason for the difference in the regressions for freezing rain and in-cloud icing, then one would expect the regression lines for the 3-mm diam cylinder for both types of icing to be quite close (see Figure 10). This is not entirely the case. Actually, the ratio of the mass of ice for freezing rain to that for in-cloud icing for a specific number of instrument cycles is not too different for both cylinder sizes. For example, at 10 cycles, the ratio of the mass of ice for freezing rain to that for in-cloud icing for the 25-mm diam cylinder is 2.24, as opposed to 2.23 for the 3-mm cylinder. At 40 cycles, the ratios are 2.85 and 2.45, respectively.

Ice accumulating on the 3-mm diam cylinder will increase its over-all dimensions, causing a decrease in collection efficiency. At the same time, the sensor on the detector maintains a constant collection efficiency. This will explain in part, the difference in the regression lines for the 3-mm cylinder in Figure 10. In addition, it appears likely that the difference in the regression line for both cylinders can be further explained by considering the freezing fraction, that is, the ratio of the amount of ice that actually freezes on the collector, to that amount which would accumulate if all the drops impinging on the collector freeze. During in-cloud icing, drops freeze quickly to the collector since the heat loss, especially the transfer of latent heat from the freezing of these small drops, is relatively rapid. The larger drops, during freezing rain, freeze more slowly. This allows part of the water to run off or be blown off the surface. The freezing fraction is influenced by the ambient temperature and the water concentration.[17] With these factors being equal, a larger surface area will allow a greater proportion of the impinging drops to freeze. This is primarily due to the increased time the drops remain on the surface and the larger ice surface to which heat can be imparted. It seems likely that, during freezing rain, many of the drops impinging on the sensor will splatter, run off, or be blown off. The rapidly expanding ice surface on the 3-mm cylinder will gradually allow a larger percentage of these drops to freeze.

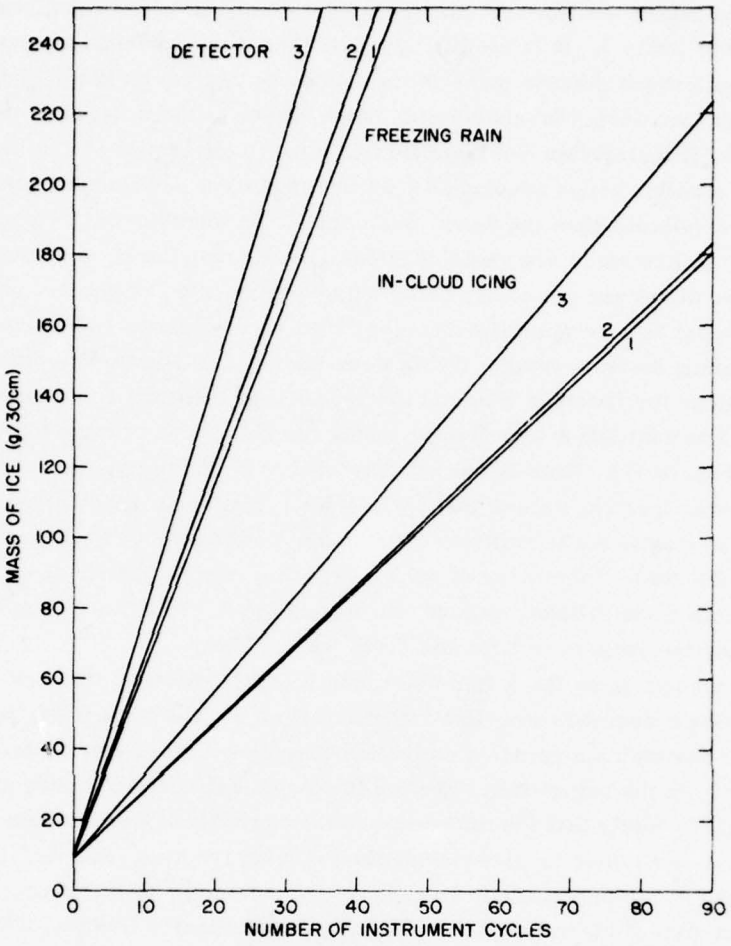


Figure 9. Least-Squares Linear Regression Lines for the Mass of Ice on the 25-mm diam Cylinder vs the Number of Detector Deicing Cycles from Information in Table 3 for Freezing Rain and In-cloud Icing

Referring back to Figure 9, one can see that the regression lines for Detector 3 have a different slope than those for Detectors 1 and 2. A representative of Rosemount Engineering Company stated that this was probably the result of an error in calibration at the factory. Detector 2, the same model used in the May 1977 tests, performed well, since ice accumulations on the mounting plate, which would have caused any interference, were removed manually.

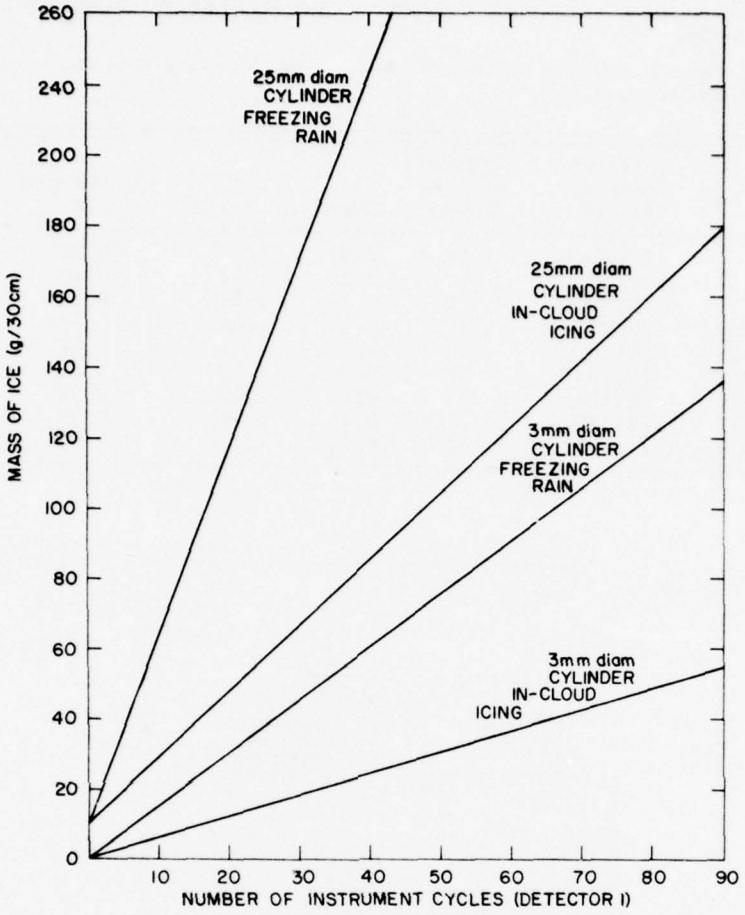


Figure 10. Least-Squares Linear Regression Lines of the Mass of Ice on the 3- and 25-mm diam Cylinder vs the Number of Detector Deicing Cycles (Detector 1) for the Freezing Rain and In-cloud Icing Tests Separately

Linear least-squares regression information for the maximum radial ice thickness (from the surface of the cylinder to the edge of the accreted ice) on the 25-mm diam cylinder versus the number of instrument cycles for each of the three detectors is contained in Table 4; also presented in Table 4 are the regressions for the in-cloud icing and freezing rain tests. The regression lines and scatter of the individual points for all tests, for the 21 freezing rain tests, and for the 21 in-cloud icing tests for detector 1 are shown in Figure 11.

Table 4. Linear Least-Squares Regression Information for the Maximum Radial Ice Thickness on the 25-mm diam Cylinder vs the Number of Instrument Cycles for Each Detector

(Results are given for all the test points and for the freezing rain and in-cloud icing conditions separately)

| Conditions | Detector Number Model | Number of Test Points | Slope | Y Intercept | Correlation (r) | SEE (mm) |
|---|---|---|---|---|---|---|
| All | 1/872DC | 42 | 0.34 | 1.88 | 0.88 | 2.0 |
| All | 2/871FA | 41 | 0.35 | 1.61 | 0.87 | 2.1 |
| All | 3/872DC | 42 | 0.44 | 1.62 | 0.90 | 1.9 |
| In-cloud icing | 1/872DC | 21 | 0.29 | 1.39 | 0.89 | 1.7 |
| In-cloud icing | 2/871FA | 20 | 0.31 | 1.19 | 0.90 | 1.6 |
| In-cloud icing | 3/872DC | 21 | 0.38 | 1.28 | 0.92 | 1.5 |
| Freezing rain | 1/872DC | 21 | 0.39 | 2.29 | 0.93 | 1.7 |
| Freezing rain | 2/871FA | 21 | 0.42 | 1.89 | 0.92 | 1.9 |
| Freezing rain | 3/872DC | 21 | 0.53 | 1.82 | 0.95 | 1.5 |

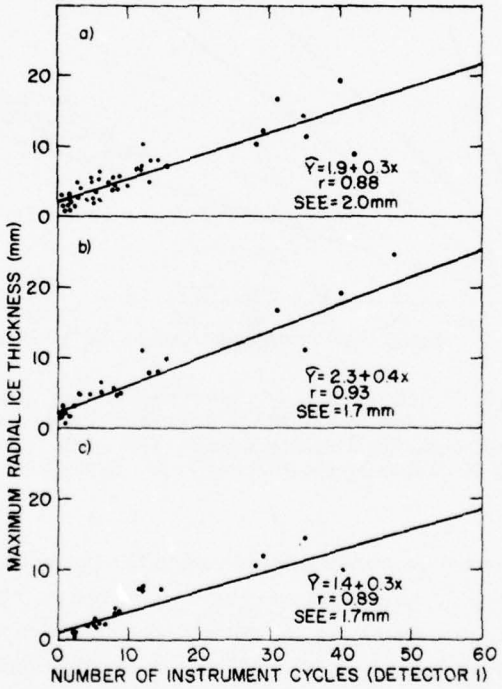


Figure 11. Maximum Radial Ice Thickness on the 25-mm diam Cylinder vs the Number of Cycles (Detector 1): (a) for all 42 one-hour tests; (b) for the 21 freezing rain tests; (c) for the 21 in-cloud icing tests

From the information in Table 4 and Figure 11, it can be seen that there is an improvement in the fit of the regression line by separating the freezing rain and in-cloud icing tests. However, the difference is not as prominent as for the mass of ice. Figure 12 shows a comparison of the least-squares regression lines of the 3- and 25-mm diam cylinders for the maximum radial ice thickness versus the number of instrument cycles. During in-cloud icing, the ice thickness is greater for the 3-mm cylinder as to be expected from icing theory. During freezing rain, however, the ice thickness is slightly greater on the 25-mm cylinder.

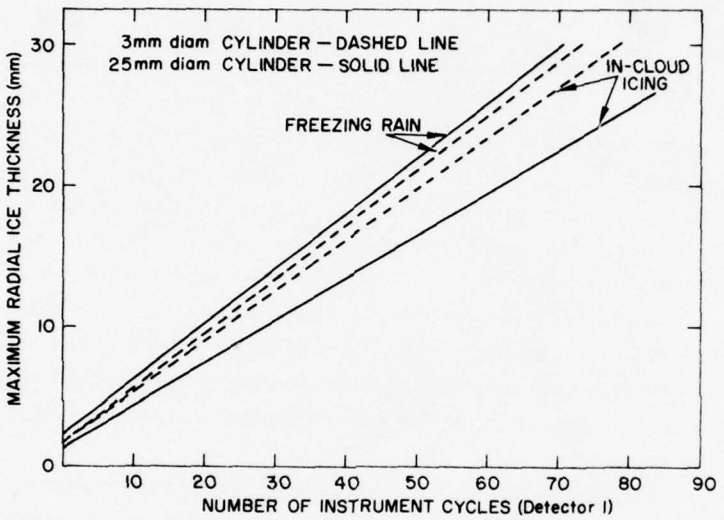


Figure 12. Least-Squares Regression Lines of the Maximum Radial Ice Thickness on the 3- and 25-mm diam Cylinders vs the Number of Instrument Cycles (Detector 1) for the Freezing Rain and In-cloud Icing Tests Separately

Another measure of the ice thickness observed after each test is the vertical dimension of the cylinder plus the ice. Subtracting the cylinder diameter from this measurement, one obtains the resultant vertical ice thickness. Table 5 contains the linear least-square regression information for this parameter versus the number of instrument cycles for detector 1. Figure 13 shows the regression lines. The results were very similar for the other two detectors.

Table 5. Linear Least-Squares Regression Information for the Resultant Vertical Ice Thickness on All Four Cylinders vs the Number of Instrument Cycles (Detector 1)

(Results are given for the freezing rain and the in-cloud icing conditions separately)

| Conditions | Cylinder diameter | Number of test points | Slope | Y Intercept | Correlation (r) | SEE (mm) |
|---|---|---|---|---|---|---|
| Freezing rain | 3 mm | 21 | 0.50 | 1.24 | 0.97 | 1.4 |
| Freezing rain | 13 | 21 | 0.45 | 0.86 | 0.95 | 1.7 |
| Freezing rain | 25 | 21 | 0.48 | 0.10 | 0.95 | 1.8 |
| Freezing rain | 50 | 21 | 0.42 | 0.26 | 0.92 | 2.0 |
| In-cloud icing | 3 | 21 | 0.16 | -0.23 | 0.93 | 0.7 |
| In-cloud icing | 13 | 21 | 0.07 | 0.03 | 0.87 | 0.4 |
| In-cloud icing | 25 | 21 | 0.00 | 0.30 | 0.06 | 0.6 |
| In-cloud icing | 50 | 21 | 0.02 | 0.36 | 0.26 | 0.9 |

From Figure 13 it can be seen that during freezing rain the accreted ice adds to the vertical dimension on all four cylinders. Also, the smaller cylinder diameters generally favor more vertical growth. During in-cloud icing the same trend is evident. However, both the 25-mm and 50-mm cylinders experience a negligible vertical growth in ice accretion. These results are consistent with theoretical concepts of collection efficiency; that is, during freezing rain, the large drops are not easily deflected, even by the 50-mm diam cylinder. During in-cloud icing, the smaller drops are deflected much more with increasing cylinder diameter. Consequently, vertical growth of the ice is less important during in-cloud icing than during freezing rain.

The relationships of cylinder size, windspeed, ambient temperature, and type and intensity of ice accretion to the measured mass and maximum radial thickness of the ice were analyzed in order to determine their relative influence. Figure 14 shows the ratio of ice thickness and mass measured on the 3-mm diam cylinder to that on the 50-mm diam cylinder versus windspeed, ambient temperature, and the type and intensity of icing. From Figure 14, it appears that the ratio of the mass of the ice accumulation on the 3-mm diam cylinder to that on the 50-mm diam cylinder shows little variation and with no apparent trend. By comparison, the ratio of ice thicknesses for the same cylinders show a great deal of variability. Most significant, though, is that during freezing rain, the ratio of the ice thicknesses for the two cylinders is frequently less than 1. The mean of the individual ratios for freezing rain is 0.90, so that the larger cylinder apparently has a greater collection efficiency. Since all of the studies on collection efficiency were carried out with cloud sized droplets, the implication here is that the theoretical relationship of the collection efficiency of objects of different sizes is limited by the drop

size; that is, once drops reach a certain mass, their inertial force is great enough so that the influence of the drag force is not sufficient to deflect a significant number of these large drops.

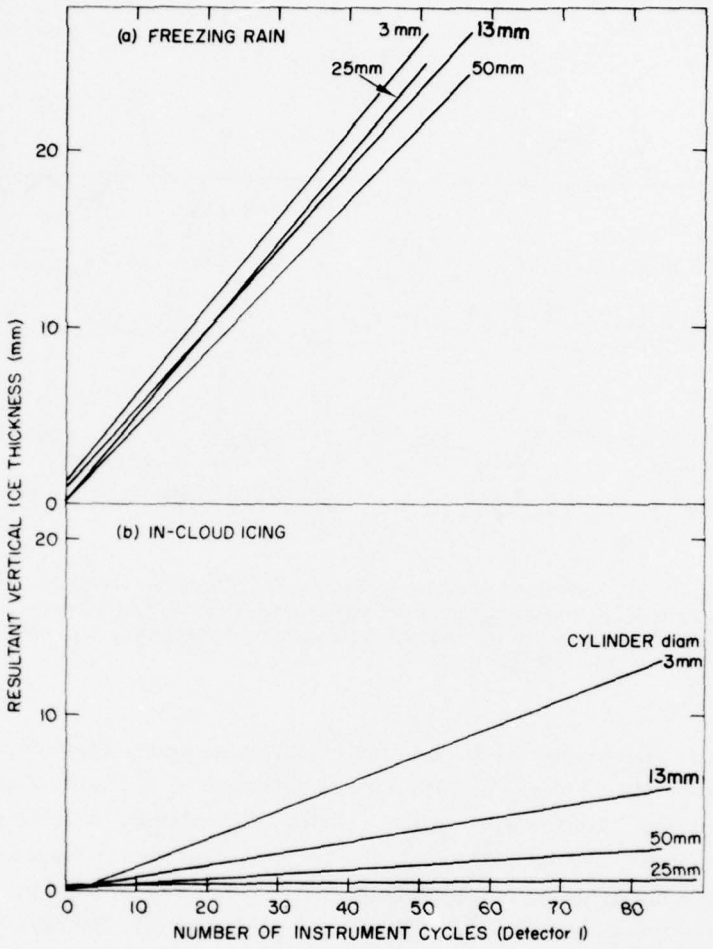


Figure 13. Least-Squares Regression Lines of the Resultant Vertical Ice Thickness vs the Number of Instrument Cycles (Detector 1) for: (a) freezing rain; (b) in-cloud icing

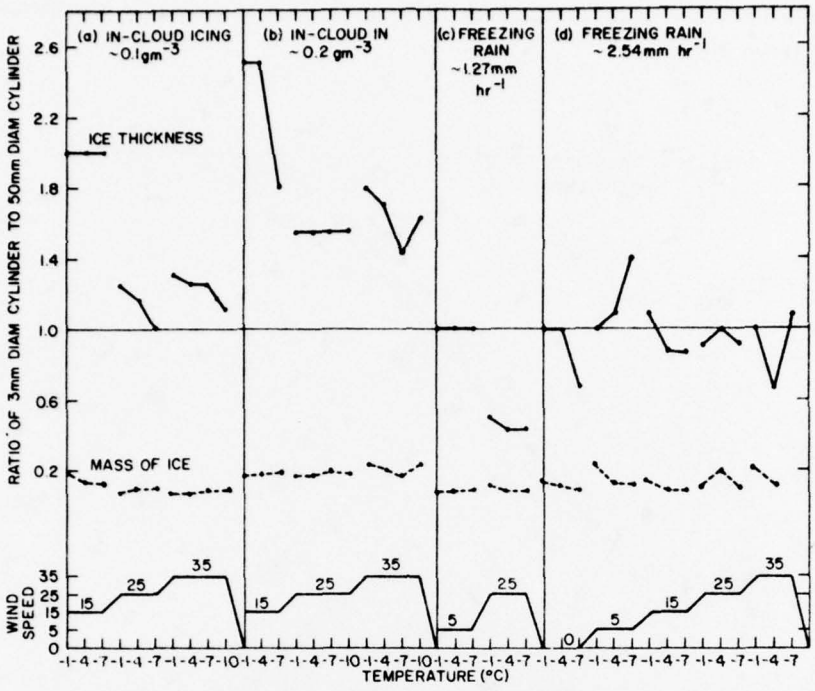


Figure 14. Ratio of Maximum Radial Ice Thickness and Mass, Measured on the 3-mm diam Cylinder to That on the 50-mm diam Cylinder vs Windspeed, Ambient Temperature, and the Type and Intensity of Icing

In order to study more completely the performance of the ice detectors, six climatic chamber tests were run with durations from 2 to 17 hours, some with varying conditions. Test conditions and results are contained in Table 6 for the in-cloud icing tests, and in Table 7 for the freezing rain tests. As a result of these longer tests, a major problem area was brought into focus. During the 15- and 17-hour freezing rain tests (test numbers 5 and 6 in Table 7), the detectors cycled erratically even though synoptic conditions remained unchanged. This was caused by melt water from the sensor accumulating on the flat surface area on the top of the strut, and held in place by surface tension. During test 6, with the temperature at -4°C, the puddle froze rapidly. The sensor, which was partially submerged in the puddle, responded by returning to the deice mode. This accounts for the large number of cycles for Detectors 1 and 3 in this test. Because of the narrow strut on Detector 2 (Model 871FA), melt water drained more readily and no puddle formed.

Table 6. Results of Long Duration Tests for In-cloud Icing

| Test Number | Conditions | | | | Mass of ice on the 25-mm diam cylinder (grams/30 cm) | Number of Cycles | | |
|---|---|---|---|---|---|---|---|---|
| | Windspeed (knots) | Temperature (°C) | Intensity ($g\ m^{-3}$) | Duration (hours) | | 1 | 2 | 3 |
| 1 | 15 | -4 | 0.2 | 1/2 | | | | |
| | 15 | -4 | 0.1 | 1/2 | | | | |
| | 25 | -4 | 0.1 | 1/2 | | | | |
| | 25 | -4 | 0.2 | 1/2 | | | | |
| | | | Total | 2 | 34.5 | 9 | 10 | 7 |
| 2 | 15 | -4 | 0.1 | 1 | | | | |
| | 15 | -7 | 0.1 | 1 | | | | |
| | 15 | -7 | 0.2 | 1 | | | | |
| | 25 | -7 | 0.1 | 1 | | | | |
| | 25 | -10 | 0.2 | 1 | | | | |
| | 35 | -10 | 0.2 | 1 | | | | |
| | | | Total | 6 | 122.8 | 61 | 68 | 64 |
| 3 | 15 | -4 | 0.2 | 6 | 64.5 | 23 | 30 | 21 |

Table 7. Results of Long Duration Tests for Freezing Rain

| Test Number | Conditions | | | | Mass of ice on the 25-mm diam cylinder (grams/30 cm) | Number of Cycles | | |
|---|---|---|---|---|---|---|---|---|
| | Windspeed (knots) | Temperature (°C) | Intensity ($mm\ hr^{-1}$) | Duration (hours) | | 1 | 2 | 3 |
| 4 | 5 | -4 | 0.10 | 1 | | | | |
| | 5 | -1 | 0.10 | 1 | | | | |
| | 15 | -1 | 0.10 | 1 | | | | |
| | 15 | -4 | 0.10 | 1 | | | | |
| | 25 | -4 | 0.05 | 1 | | | | |
| | | | Total | 5 | 308.6 | 34 | 37 | 29 |
| 5 | 5 | -1 | 0.10 | 15 | 539.0 | 39 | 40 | 58 |
| 6 | 5 | -4 | 0.05 | 17 | 156.6 | 115 | 28 | 124 |

During test 5, with the temperature at -1°C, the puddle was slow to freeze. It is not apparent what physical effect this had on the cycling of the detector. Deicing intervals were irregular; however, excessive cycling did not occur as with the case of the 17-hour test. Figure 15 shows the least-squares linear regression lines for the mass of ice on the 25-mm diam cylinder versus the number of instrument cycles for each detector (from Figure 9). The values for the mass of ice on the 25-mm diam cylinder versus the number of cycles for each detector for the long duration tests in Tables 6 and 7 are also shown. Since the number of cycles for detectors 1 and 3 in test number 6 are not representative, they have not been plotted.

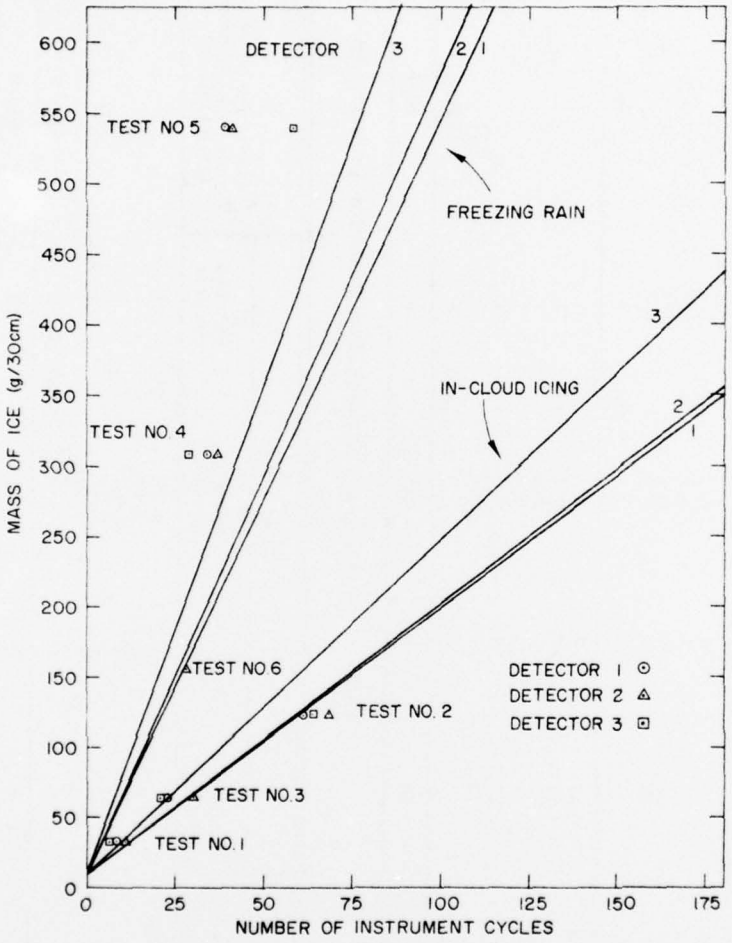


Figure 15. Least-Squares Linear Regression Lines for the Mass of Ice on the 25-mm diam Cylinder vs the Number of Instrument Cycles for Each Detector from Figure 9. Values for the long duration tests are outlined with a circle for Detector 1, a triangle for Detector 2, and a square for Detector 3

Table 8 contains the percentage difference between the mass of ice measured on the 25-mm diam cylinder in the long duration tests and that estimated from the regression lines for each detector. The percentage differences are notably larger for the freezing rain tests. Also there is a tendency for the regression lines for freezing rain to underestimate the mass of ice, which happened in all instances but one. The mean of the absolute values of these differences for freezing rain is 37 percent; for in-cloud icing it is 18 percent. One explanation for this is the growth in the size of the cylinder plus ice, especially in the vertical plane, during freezing rain. As indicated previously, the larger the cylinder, the greater the mass of accumulated ice. Evidently, using the regression lines based on the 1-hour tests can lead to significant underestimates of the mass of ice during prolonged severe icing such as our long duration tests. This is not a problem during in-cloud icing because vertical growth on the cylinder is small and the frontal projection remains effectively unchanged.

Table 8. Percentage Difference Between the Mass of Ice Measured on the 25-mm diam Cylinder in the Long Duration Tests and That Estimated From the Regression Lines for Each Detector*

| Test Number | Type of icing | Detector | Percentage Difference 1 | 2 | 3 |
|---|---|---|---|---|---|
| 1 | In-cloud | | 30 | 25 | 35 |
| 2 | In-cloud | | -2 | -12 | -24 |
| 3 | In-cloud | | 22 | -3 | 9 |
| 4 | Freezing rain | | 60 | 42 | 48 |
| 5 | Freezing rain | | 46 | 29 | 31 |
| 6 | Freezing rain | | ... | -6 | ... |

*Negative sign indicates that the measured mass is less than that obtained from the regression line.

### 5.3 Evaluation of Test Results

The difficulties encountered during our original test period, especially with regard to the failure of the Rosemount Model 872DC ice detectors, precluded our judging the utility of this ice detector as a potential meteorological instrument for objectively measuring ice accretion. However, the use of a substitute detector (Model 871FA) showed that the system was promising, in spite of errors resulting from uneven icing on components used to measure icing amounts. With the experience gained from the original tests, and the return of the ice detectors which were more adaptable to our goals, we were able to conduct a more effective second test

program. Because of this, the data collected during the two test periods were not combined. However, one of the substitute detectors was used in the second test period and, for comparison, Figure 16 shows the regression lines for the mass of ice measured on the 50-mm diam cylinder versus the number of instrument cycles during freezing rain tests for the two test periods.

The complexity of ice accretion processes is evident from the theoretical discussion in Section 2, and from the results of our tests. However, the 872DC detectors were highly correlated with measurements of ice mass and thickness on cylinders, regardless of the rate of accretion (which includes the influence of windspeed, ambient temperature and precipitation rate). Although instrument response was sensitive to the type of ice accretion due to differences in drop sizes, this should not be a major problem in actual use because drop sizes are categorized by synoptic conditions related to the type of icing.

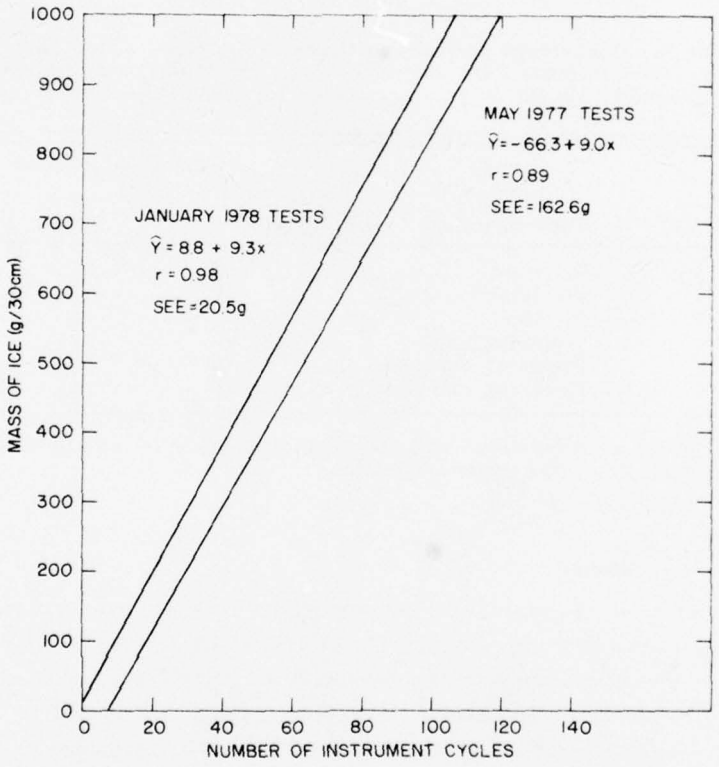


Figure 16. Comparison of the Linear Least-Squares Regression Lines of the Mass of Ice Measured on the 50-mm diam Cylinder vs the Number of Instrument Cycles (Model 871FA, Serial Number 34) for the Two Test Periods

## 6. APPLICATION

The application of ice accretion measurements is primarily in the area of environmental design criteria. The two aspects of ice accretion that are important in this regard are: (1) wind loading due to the increased surface area of the structure as a result of accumulated ice; and (2) the mass of ice on the structure.

The determination of surface area is necessary for the engineer to calculate the force of the design windspeed on the structure. This determination is straightforward when ice is not present, since the surface area can be easily calculated, and data on windspeed distributions are available for a large number of locations. When ice is present, it is necessary to know the distribution of concurrent observations of windspeed and ice thickness. During natural ice accretion, ice thickness varies and assumes a variety of shapes, depending on the orientation and size of the collecting surface and the synoptic conditions. This can be further complicated by the presence of icicles, which are not usually included in measurements of ice thickness.

During the climatic chamber tests, measurements were made of the ice thickness in the vertical as well as the maximum radial ice thickness. However, these measures of thickness are dependent on cylinder orientation and the wind direction. The term "radial ice thickness" has frequently been used in the literature to describe ice thickness.[4] This term implies a uniform coating of ice on a cylinder such that the thickness of the ice is the radius of the cylinder and ice minus the radius of the cylinder. The concept is attractive in its simplicity, even though it does not describe the shape of accreted ice actually occurring in nature. This approach to ice thickness was explored using the data from the climatic chamber tests.

Consider a cylinder with length L and radius $r_2$. Let $r_1$ be the radius of the cylinder plus a uniform coating of ice on the cylinder. Then

$$T = r_1 - r_2 \tag{7}$$

where T is the theoretical radial ice thickness. From simple geometry, the volume of ice $V_I$ can be calculated from

$$V_I = \pi L (r_1^2 - r_2^2) , \tag{8}$$

so that

$$r_1 = \sqrt{\frac{V_I}{\pi L} + r_2^2} . \tag{9}$$

Also,

$$V_I = \frac{M_I}{\rho_I} \tag{10}$$

where $M_I$ is the mass of ice on the cylinder and $\rho_I$ is the ice density. Combining Eqs. (9) and (10) and substituting for $r_I$ in Eq. (7), one obtains

$$T = \sqrt{\frac{M_I}{\rho_I \pi L} + r_2^2} - r_2 \tag{11}$$

The actual increase in the thickness of the cylinder plus ice is 2T. For a 2.54 cm diam cylinder with a length of 30.48 cm (1 ft), and assuming an ice density of 0.9 g $cm^{-3}$, the theoretical increase in the thickness of the cylinder T′ is

$$T' = 2\left(\sqrt{\frac{M_I}{86.18} + 1.61} - 1.27\right) \tag{12}$$

The least-squares linear regression of T′, calculated using the mass of ice on the 25-mm diam cylinder, versus the resultant vertical ice thickness on the same cylinder for the 21 January 1978 freezing rain tests is shown in Figure 17. Figure 18 shows the least-squares linear regression of T′ versus the maximum radial ice thickness for the same tests. It can be seen that there is a significant relationship between T′ and both the resultant vertical ice thickness and the maximum radial ice thickness. However, if Eq. (11) provided the best possible results, the regression lines in Figures 17 and 18 would have an intercept of zero and a slope of 1; that is,

$$\hat{Y} = T' . \tag{13}$$

If we use the value 0.8 g $cm^{-3}$ for the ice density, then

$$T' = 2\left(\sqrt{\frac{M_I}{76.6} + 1.61} - 1.27\right) \tag{14}$$

for the 25-mm diam cylinder. The least-squares linear regression lines for T′ calculated from Eq. (14) versus the resultant vertical ice thickness, and also versus the maximum radial ice thickness are shown in Figure 19. Equation (13), shown as a dashed line, provides a good estimate of the ice thickness. The use of 0.8 g $cm^{-3}$ for the density of ice formed by freezing rain is reasonable, since there are usually some air bubbles trapped in the ice and the actual density would be in the range of 0.8 to 0.9 g $cm^{-3}$. The density of pure ice is 0.917 g $cm^{-3}$. Therefore, Eq. (11)

can be used to calculate the radial ice thickness from the mass of ice on the 25-mm diam cylinder due to freezing rain, assuming an ice density of 0.8 g $cm^{-3}$. Analyses of the ice thickness on the 3-, 13-, and 50-mm diam cylinders using Eq. (11) with an ice density of 0.8 g $cm^{-3}$ yielded similarly good results.

For in-cloud icing, a density of 0.6 g $cm^{-3}$ was used in Eq. (11) resulting in the expression

$$T = \sqrt{\frac{M_I}{57.45}} + 1.61 - 1.27 . \qquad (15)$$

This density is the approximate lower limit for hard rime, and its use will maximize the theoretical radial ice thickness calculated using Eq. (11). Ice with a lower density has little adhesive strength; it is not an important design consideration, since it would be blown off by strong winds. The least-squares linear regression of T′ (T′ = 2T) versus the maximum radial ice thickness on the 25-mm diam cylinder for the 21 in-cloud icing tests from the January 1978 test period is presented in Figure 20. Equation (13) is also shown as a dashed line. For the same tests, the regression line for the resultant vertical ice thickness on the 25-mm diam cylinder versus T′ is not shown because the resultant vertical thickness was close to zero, although some vertical growth occurred on the smaller (3- and 13-mm diam) cylinders (see Figure 13b). The increased surface area due to the maximum radial ice thickness depends on the orientation of the ice coated structure to the wind. The use of Eq. (15) to calculate the theoretical radial ice thickness on the 25-mm diam cylinder for in-cloud icing is a compromise for all possible orientations to the wind.

A suggested method for utilizing the output of the 872DC ice detector in actual use would be to use the number of recorded deicing cycles to determine the mass of ice per unit length on a cylinder. If we adopt the mass of ice per 30.5 cm (1 ft) on the 25-mm diam cylinder as a basis for describing ice accretion observations, then the mass of ice on the 3-, 13-, and 50-mm diam cylinders can be determined using the factors in Table 9. The radial ice thickness can then be calculated for each cylinder size using Eq. (11) with the appropriate ice density for the type of icing.

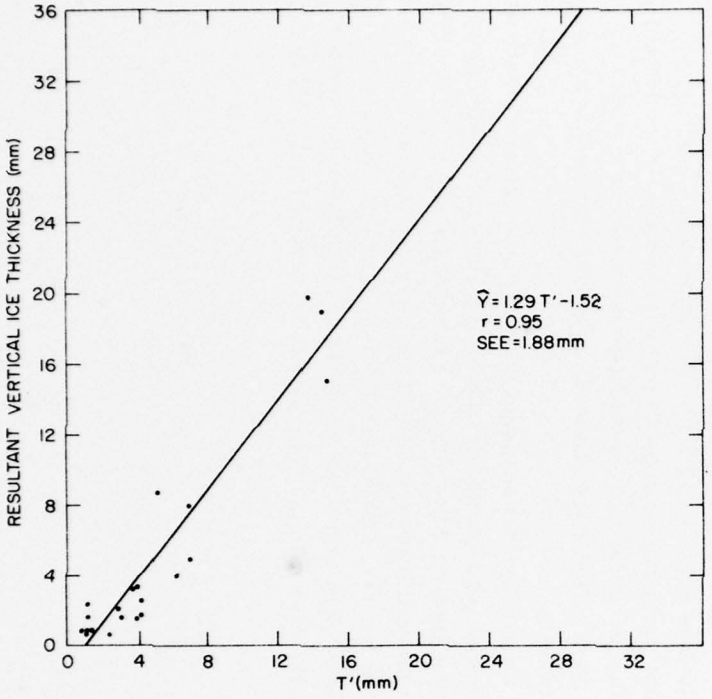


Figure 17. Least-Squares Linear Regression of T′ vs the Resultant Vertical Ice Thickness for the January 1978 Freezing Rain Tests

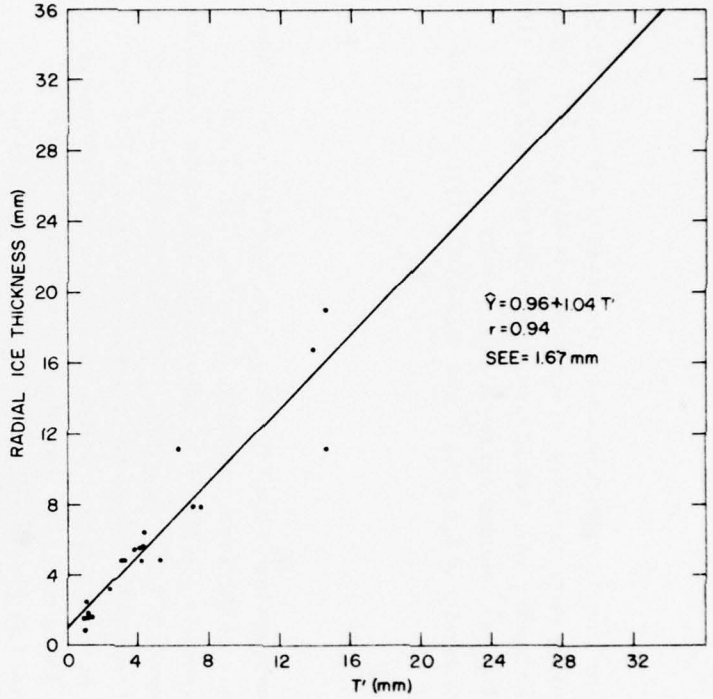


Figure 18. Least-Squares Linear Regression of T′ from Eq. (12) vs the Maximum Radial Ice Thickness for the January 1978 Freezing Rain Tests

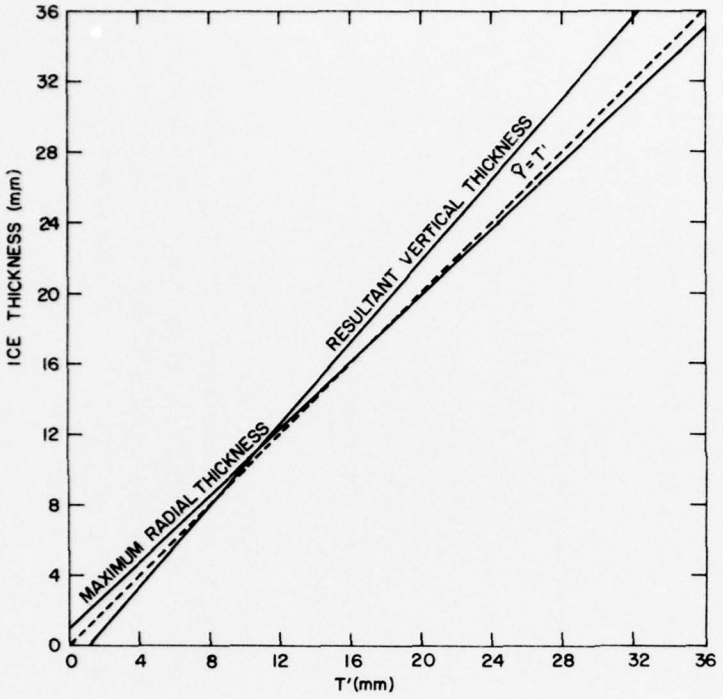


Figure 19. Least-Squares Linear Regression Lines of the Resultant Vertical Ice Thickness and the Maximum Radial Ice Thickness vs T′ from Eq. (14) for the January 1978 Freezing Rain Tests. $\hat{Y} = T'$ is represented by the dashed line

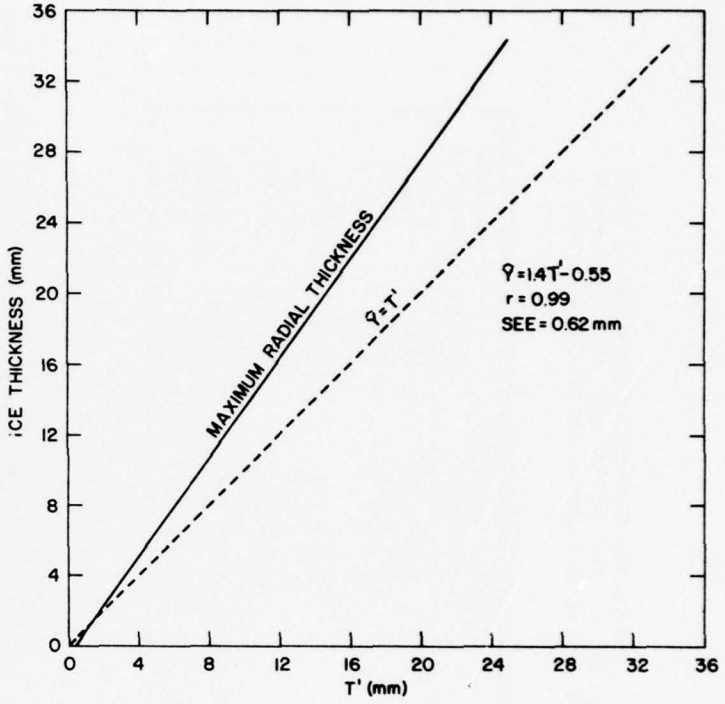


Figure 20. Least-Squares Linear Regression of the Maximum Radial Thickness vs T′ for the January 1978 In-cloud Icing Tests. $\hat{Y} = T'$ is represented by the dashed line

Table 9. Mean and Standard Deviation of the Ratios of the Mass of Ice on the 3-, 13-, and 50-mm diam Cylinders to That on the 25-mm diam Cylinder for the January 1978 Test Period

| Category | Cylinder diameter (mm/inches) | Mean | Standard Deviation |
|---|---|---|---|
| In-cloud icing | 3.2 / 1/8 | 0.21 | 0.059 |
| In-cloud icing | 12.7 / 1/2 | 0.59 | 0.062 |
| In-cloud icing | 50.8 / 2 | 1.47 | 0.116 |
| Freezing rain | 3.2 / 1/8 | 0.18 | 0.041 |
| Freezing rain | 12.7 / 1/2 | 0.54 | 0.056 |
| Freezing rain | 50.8 / 2 | 1.65 | 0.091 |
| Both combined | 3.2 / 1/8 | 0.20 | 0.054 |
| Both combined | 12.7 / 1/2 | 0.57 | 0.063 |
| Both combined | 50.8 / 2 | 1.56 | 0.139 |

## 7. CONCLUSION

Based on the analyses of the climatic chamber test data, the Rosemount Model 872DC ice detection system has proved an effective tool for determining the mass and thickness of ice accretion on cylinders. At the time of this writing, several items remain to be resolved before utilizing the 872DC ice detectors for icing observations. They are as follows:

1. Modification of the Ice Detector

It was pointed out in the discussion of the long duration tests that melt water accumulated on the flat surface area on top of the strut on which the sensor is located. This altered the response of the detectors during prolonged icing with light winds (≤ 15 kt). At higher windspeeds, the melt water was blown off. This problem could be eliminated by tapering the top of the strut to facilitate drainage. Representatives at Rosemount were consulted about this, and they felt that the modification could be accomplished at a reasonable cost per detector, depending on the number of modified detectors ordered.

2. Detector Calibration

It was apparent from the analysis of the climatic chamber test data that there was a significant difference in the response time of the 872DC detectors. A representative of Rosemount stated that the difference in response time between detectors can vary by as much as 15 to 25 percent. He indicated that greater attention to calibration at the factory should reduce the variance to about 10 percent, possibly less.

3. Proper application of detector output

The major factor affecting the detector response, other things being equal, is due to the type of icing. This is a result of differences in drop size. The regression lines for the mass of ice versus the number of cycles for freezing rain and in-cloud icing represent limits of the detector response to icing. What remains to be evaluated is the response of the detector to icing conditions with drop sizes between those for in-cloud icing and freezing rain, in particular freezing drizzle, or a mixture of freezing rain and drizzle. This is not as formidable a problem as it might seem, because each type of icing is a discrete entity that can be easily identified by an observer. What remains to be determined is a method for interpolating the detector response for conditions, such as freezing drizzle, which have drop sizes between in-cloud icing and freezing rain. Also, the long duration tests indicated that the regression lines for freezing rain underestimated the mass of ice during prolonged severe icing. Observations of the detectors in the natural environment should provide a better understanding of what adjustments have to be made to these relationships. Section 8 describes a program for this purpose that is currently under way at AFGL.

4. Keeping track of residual ice

The main emphasis in this report has been on observing the quantity of ice resulting from a period of ice accretion. In engineering design, it is also important to know the distribution of concurrent observations of wind and ice. Since the strongest windspeeds could occur subsequent to the period of icing, especially in cold locations, it is necessary to develop a method for determining the quantity of residual ice remaining on structures after the icing has stopped. Techniques for doing this will be explored during our tests in the natural environment.

## 8. ON-GOING EFFORTS

A program is currently under way at Air Force Geophysics Laboratory whereby Rosemount 872DC ice detectors will be mounted on a stand and installed at four sites in the northeastern United States. Two of the sites will be at Hanscom AFB, and Blue Hill Observatory, both in eastern Massachusetts. Both sites will be operational by November 1979. On each stand a cylinder 30.5 cm in length with a diameter of 25 mm will be mounted on a vane 90 cm from the ice detector. The cylinder, which will be kept normal to the wind direction, will be removable so that the mass of ice can be determined.

Detector output will be compared with ice measurements on the cylinder, in order to evaluate the regression lines of the number of instrument deicing cycles versus the mass and thickness of ice determined from the climatic chamber test data.

## References


1. Rudneva, A.V. (1961) Glazed Frost and Ice Formation on Cables Within the Territory of the USSR, Special Translation, No. ATD U-64-47, Aerospace Technology Division, Library of Congress, 28 July 1964.

2. Austin, J.M., and Hensel, S.L. (1956) Analysis of Freezing Precipitation Along the Eastern North American Coastline, MIT, Lincoln Laboratory, Tech. Rpt. No. 112, 23 March 1956, 46 pp.

3. Bennett, I. (1959) Glaze, Its Meteorology and Climatology, Geographical Distribution and Economic Effects, Tech. Rpt. EP-105, Quartermaster Research and Engineering Center, Envir. Prot. Res. Div., Natick, Massachusetts.

4. Tattelman, P., and Gringorten, I.I. (1973) Estimated Glaze Ice and Wind Loads at the Earth's Surface for the Contiguous United States. AFCRL-TR-73-0646, AD A775068, 16 October 1973, 35 pp.

5. McKay, G.A., and Thompson, H.A. (1969) Estimating the hazard of ice accretion in Canada from climatological data, J. Appl. Meteorol. 8(No. 6):927-935.

6. Bilello, M.A. (1967) Survey of Frozen Precipitation in Urban Areas as Related to Climatic Conditions, Cold Regions Research and Engineering Laboratory, Tech. Rpt. No. 162, May 1967, 30 pp.

7. Lenhard, R.W. (1955) An indirect method for estimating the weight of glaze on wires, Bull. Am. Meteorol. Soc. 36(No. 1):1-5, January 1955.

8. Chaine, P.M., Verge, R.W., Castonguay, G., and Gariepy, J. (1974) Wind and Ice Loading in Canada, Industrial Meteorology - Study II, Atmospheric Environment Service, Toronto, Canada, 6 pp.

9. Chaine, P.M., and Skeates, P. (1974) Wind and Ice Loading Criteria Selection, Industrial Meteorology - Study III, Atmospheric Environment Service, Toronto, Canada, 14 pp.

10. Kuroiwa, Daisuke (1965) Icing and Snow Accretion on Electric Wires, Research Report 123, Cold Regions Research and Engineering Laboratory, Hanover, N.H., January 1965, 10 pp.

## References


11. Macklin, W.C. (1961) The density and structure of ice formed by accretion, Quart. J. Roy. Meteorol. Soc. 88:30-50.

12. Bryson, R.A., and Hare, F.K. (1974) Climates of North America, World Survey of Climatology, Vol. II, Elsivier Scientific Publishing Co., Amsterdam, 420 pp.

13. Bilello, M.A. (1971) Frozen Precipitation: Its Frequency and Associated Temperatures, Cold Regions Research and Engineering Laboratory, Hanover, N.H., 13 pp.

14. Young, W.R. (1978) Freezing Precipitation in the Southeastern United States, Master's Thesis, Texas A&M University, Report Number CI 78-24, College Station, Texas, 123 pp.

15. Mason, B.J. (1971) The Physics of Clouds, 2nd ed., Oxford University Press, London, England.

16. Chaine, P.M., and Castonguay, G. (1974) New Approach to Radial Ice-Thickness Concept Applied to Bundle-Like Conductors, Industrial Meteorology - Study IV, Atmospheric Environment Service, Toronto, Canada, 11 pp.

17. Stallabrass, J.R., and Hearty, P.F. (1967) The Icing of Cylinders in Conditions of Simulated Freezing Sea Spray, National Research Council of Canada, Ottawa, Canada, 50 pp.

18. Hill, A.N. (1973) An Objective Observation Technique for Freezing Precipitation, Laboratory Report No. 7-73, Sterling Research and Development Center, Sterling, Virginia.

19. Chaine, P.M., and Waymann, A.R. (1974) A Preliminary Performance Assessment of Rosemount Ice Detectors, Department of Environment, Atmospheric Environment Service, Toronto, Canada, 4 pp.

20. Best, A.C. (1949) The size distribution of raindrops, Quart. J. Roy. Meteorol. Soc. 76:16-36.